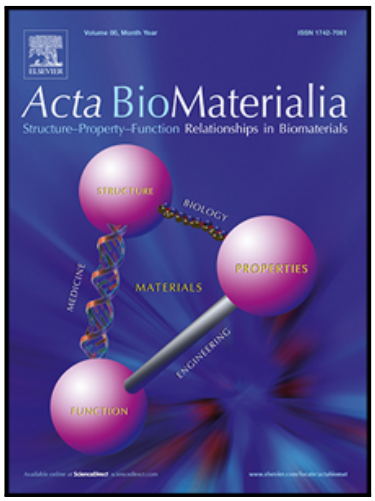

Multi-material additive manufacturing technologies for Ti-, Mg-, and Fe-based biomaterials for bone substitution

N.E. Putra , M.J. Mirzaali , I. Apachitei , J. Zhou , A.A. Zadpoor

PII: S1742-7061(20)30178-1
DOI: https://doi.org/10.1016/j.actbio.2020.03.037
Reference: ACTBIO 6655

To appear in: *Acta Biomaterialia*

Received date: 22 January 2020
Revised date: 8 March 2020
Accepted date: 26 March 2020

Please cite this article as: N.E. Putra , M.J. Mirzaali , I. Apachitei , J. Zhou , A.A. Zadpoor , Multi-material additive manufacturing technologies for Ti-, Mg-, and Fe-based biomaterials for bone substitution, *Acta Biomaterialia* (2020), doi: https://doi.org/10.1016/j.actbio.2020.03.037

Review article

Multi-material additive manufacturing technologies for Ti-, Mg-, and Fe-based biomaterials for bone substitution

N.E. Putra, M.J. Mirzaali, I. Apachitei, J. Zhou, A.A. Zadpoor

Department of Biomechanical Engineering, Faculty of Mechanical, Maritime, and Materials Engineering, Delft University of Technology, Mekelweg 2, 2628 CD Delft, The Netherlands

Abstract

The growing interest in multi-functional metallic biomaterials for bone substitutes challenges the current additive manufacturing (AM, =3D printing) technologies. It is foreseeable that advances in multi-material AM for metallic biomaterials will not only allow for complex geometrical designs, but also improve their multi-functionalities by tuning the types or compositions of the underlying base materials, thereby presenting unprecedented opportunities for advanced orthopedic treatments. AM technologies are yet to be extensively explored for the fabrication of multi-functional metallic biomaterials, especially for bone substitutes. The aim of this review is to present the viable options of the state-of-the-art multi-material AM for Ti-, Mg-, and Fe-based biomaterials to be used as bone substitutes. The review starts with a brief review of bone tissue engineering, the design requirements, and fabrication technologies for metallic biomaterials to highlight the advantages of using AM over conventional fabrication methods. Five AM technologies suitable for metal 3D printing are compared against the requirements for multi-material AM. Of these AM technologies, extrusion-based multi-material AM is shown to have the greatest potential to meet the requirements for the fabrication of multi-functional metallic biomaterials. Finally, recent progress in the fabrication of Ti-, Mg-, and Fe-based biomaterials including the utilization of multi-material AM technologies is reviewed so as to identify the knowledge gaps and propose the directions of further research for the development of multi-material AM technologies that are applicable for the fabrication of multi-functional metallic biomaterials.

Statement of significance

Addressing a critical bone defect requires the assistance of multi-functional porous metallic bone substitutes. As one of the most advanced fabrication technology in bone tissue engineering, additive manufacturing is challenged for its viability in multi-material fabrication of metallic biomaterials. This article reviews how the current metal additive manufacturing technologies have been and can be used for multi-material fabrication of Ti-, Mg-, and Fe-based bone substitutes. Progress on the Ti-, Mg-, and Fe-based biomaterials, including the utilization of multi-material additive manufacturing, are discussed to direct future research for advancing the multi-functional additively manufactured metallic bone biomaterials.

Keywords: Additive manufacturing; multi-material; metal; biomaterial; bone implant.

1. INTRODUCTION

1.1 Bone tissue engineering

Bone takes part in the key functions of the human body for locomotion, protection of soft tissues and organs, and mineral homeostasis [1]. It has two basic structures (Figure 1): the inner part (*i.e.*, the cancellous bone) also called spongy bone with 50 – 90% porosity and the outer part (*i.e.*, the cortical bone) also called compact bone with only ~10% porosity [2]. Due to the structural complexity of bone at different length scales, its mechanical properties vary over wide ranges, with the compressive yield strengths between 0.5 and 200 MPa and Young's moduli between 0.5 and 20 GPa [3].

Bone adapts to mechanical loading and heals itself when damaged at a small scale through a dynamic process of remodeling, through which old, microcracked bone is resorbed

and replaced by new bone [4]. Despite being able to regenerate, bone loss from traumas or diseases often leads to non-unions and critical-size bone lesions (*i.e.*, > 5 cm, *e.g.*, in the femur and tibia [5]). A critical-size bony lesions is defined as a lesion that cannot be healed naturally during the patient's lifetime [6]. In such cases, bone replacements are necessary.

Until today, autografts, or bone replacements collected from and implanted in the same person, remain the gold standard of the clinical treatments of critical-size bony lesions [7]. However, the volume of autografts that can be harvested to replace critical-size bony lesions, for example, from the posterior iliac crest, is limited to 33.82 cm^3 [8], while the volume of tibia defects may amount to 122 cm^3 [9]. Although allografts (*i.e.*, bone replacements from donors) can compensate the shortcomings of autografts, the risks of disease transmission as well as immunogenic incompatibility pose other types of challenges. Driven by the need to provide an alternative bone replacement approach, bone tissue engineering, which focuses on regenerating bone tissue using synthetic biomaterials, has shown promising progress in the reconstruction of large-scale bony lesions [10].

1.2 Metallic biomaterials for load-bearing bone substitutes

Ideal synthetic biomaterials for bone substitutes must be biocompatible and designed to mimic the extracellular matrix of the natural bone. They should provide bone regeneration environment, facilitate complete bone regeneration, withstand dynamic mechanical loading, and degrade along with the formation of new bone [11]. A successful bone substitute first allows mesenchymal stem cells (MSCs) to adhere onto its surface and differentiate into bone cells, followed by inward mineralization [12]. In the design of an ideal bone substitute, the mechanical properties, pore sizes, pore distribution, porosity, surface characteristics, and biodegradability of the biomaterial should all be taken into consideration.

Synthetic bone substitutes can be made using metallic biomaterials, bioceramics, biopolymers, or composite biomaterials. Metallic biomaterials have been widely used for

functional and load-bearing bone substitutes due to their mechanical properties that are superior to those of bioceramics, biopolymers and composite biomaterials. Most of bulk metals, however, are known for having mechanical properties that are much higher than those of the native bone, which induces bone tissue resorption after implantation as a result of stress shielding [13]. But, the excessively high mechanical properties of metals can be tuned by increasing their porosity. Increasing the porosity of metallic biomaterials can not only reduce their mechanical properties but also improves their permeability for cells and nutrients and facilitates angiogenesis and bone ingrowth [14]. The porosity of metallic biomaterials should be at least 50% while pore sizes > 300 μm are recommended to ensure better progress of the bone tissue regeneration process [15,16]. The porous design of metallic biomaterials should be tailored to ensure an optimum trade-off between the mechanical properties for load bearing and the porous structure needed for vascularization.

In addition, the surface of metallic biomaterials must be osteoconductive to promote adhesion, proliferation, and differentiation of the relevant cells such as MSCs. An osteoconductive surface can be obtained through generating certain surface characteristics, such as surface roughness and curvature. As bone tissue regeneration occurs more likely on concave surfaces as compared to convex or planar surfaces, large concave surface curvatures are preferred for an enhanced growth rate [17]. Moreover, nanofeatures and surface nanotopography can also induce the osteogenic differentiation of MSCs and encourage osteoblasts adhesion [18–20].

At the early stage of bone defect regeneration, the entire mechanical support relies on the implanted biomaterial. The mechanical integrity of the biomaterials should be sustained for about 3 to 12 weeks to support the upper limb healing process, while the lower limb requires approximately 12 to 24 weeks [21]. As the regenerated bone slowly regains its strength, the biomaterial is allowed to degrade gradually. Therefore, the biodegradation rate

of metallic bone substitutes should be adjusted such that the loss in the load-bearing capacity of the implanted biomaterial is balanced by the gain in the structural integrity of the bone. Furthermore, the biodegradation products must be delivered in acceptable quantities and cytotoxicity levels to ensure that they are tolerated by the human body.

With all the requirements for ideal bone substitutes fulfilled, the regeneration of bony lesions assisted by metallic biomaterials could result in healthy and functional bone. To obtain such ideal biomaterials, advanced fabrication technologies that enable the precise arrangement and control of complex geometries are required.

1.3 Fabrication technologies for metallic biomaterials used as bone substitutes

Over the years, porous metallic biomaterials have been produced using conventional fabrication technologies, mostly based on powder metallurgy, such as metal injection molding [22] or the space-holder method [23,24]. Even with the remarkable progress made in these fabrication technologies, certain limitations, such as the impossibility to control the geometry and distribution of pores precisely, as well as dimensional inaccuracies, remain.

Additive manufacturing (AM) has recently emerged as a powerful method for the fabrication of biomaterials, including metallic biomaterials aimed for bone tissue regeneration [25]. AM technologies enable high-precision fabrication with high flexibility in the internal and external macro- and micro-architecture of orthopedic implants [26]. Through controlled AM fabrication processes, geometrical and topological porous characteristics of metallic biomaterials can be precisely tuned, leading to improved bone-mimicking mechanical properties [27,28], altered biodegradation kinetics [29,30], enhanced bone tissue regeneration rates [31–33] and the formation of an extensive, interconnected osteocyte lacuno-canalicular network [34,35]. However, some other properties, including hardness, wear resistance, anti-ferromagnetic properties, or antibacterial properties, cannot be simply

adjusted through geometrical design, as they require the adjustments of the properties of the underlying base material(s) prior to AM processing.

As for the biocompatibility, most metallic biomaterials have a relatively low intrinsic osteogenic and osteoimmunomodulation potential as compared with, for example, Ca-P-based bioceramics [36]. Their presence as foreign body objects is often a risk factor for prolonged chronic inflammation [37]. The high surface area to volume ratio of porous AM metallic biomaterials raises another challenge in preventing bacteria colonization. These issues are currently being addressed by taking an additional post-AM step of surface biofunctionalization to add bioactive agents to the porous surfaces in order to improve the performance of AM biomaterials including their osteogenic properties, and to prevent infection [38].

The existing technologies for the fabrication of multi-functional porous AM metallic biomaterials strongly rely on the availability of pre-alloyed materials and the post-AM surface biofunctionalization, thus, being a two-step process. There is a strong need to upgrade the AM technologies so that they can realize the desired spatial distribution and bonding of multiple materials, thereby enabling the *in situ* synthesis of multiple materials in one single AM process.

Utilizing multi-material AM technologies will enable the fabrication of multi-functional porous AM metallic biomaterials with region-specific performance such that the material types and compositions can be specifically placed at different scales within the biomaterials design. The mechanical properties of porous AM metallic biomaterials, including hardness, can be realized, in accordance with those of cortical and trabecular bone by changing not only the porosity but also the material types or compositions. Enhanced osteoconductivity and antibacterial properties with appropriate inflammatory responses can be obtained through the right compositions and distributions of bioactive agents on the metallic surfaces. Varying the

compositions and types of materials that have distinct biodegradation properties, for example, from bio-inert or slowly biodegrading biomaterials to fast biodegrading materials, will create complex profiles of biomaterials properties over time, as clinically required.

Despite the fact that numerous properties of porous AM metallic biomaterials can be improved by using multi-material metallic AM technologies, the currently available literature on these technologies is relatively scarce [39]. Recent literature on the AM technologies for bone tissue engineering is mainly focused on the commercially available AM processes and the choices of existing biomaterials, including biocompatible metals [40–44], and geometrical and topological designs of porous AM metallic biomaterials [45–49] in relation to their mechanical and biological performance. Regarding the multi-material AM technologies, multi-material polymers are advancing the frontiers of multi-material AM concepts due to the relative simplicity of the involved processes and the compatibility of those materials with multiple AM technologies [50]. *In situ* multi-material AM for metals and metal-ceramic composites have been mainly reviewed for industrial applications, such as in aerospace and automotive applications [51–53], but not specifically for biomedical applications.

In this review, we present the prospects of using the currently available metallic AM technologies for *in situ* or *ex situ* multi-material fabrication of multi-functional Ti-, Mg-, Fe-based bone substituting biomaterials. The key principle of each of the AM technologies as well as their its advantages and limitations for multi-material fabrication are described, analyzed, and compared. Recent research on Ti-, Mg-, and Fe-based biomaterials and the (multi-material) AM technologies for these biomaterials is also reviewed. Finally, the current challenges and future perspectives in metallic multi-material AM technologies are provided.

2. MULTI-MATERIAL METALLIC AM TECHNOLOGIES

To build multi-functional porous AM metallic biomaterials using multi-material AM technologies, multiple materials must be delivered during the fabrication processes, and

strong bonding between biomaterials of different types or compositions must be ensured. Multiple material delivery systems and their bonding processes vary, depending on the particular AM technology used. Meeting these two requirements is essential for successful multi-material fabrication, as they strongly influence the performance of the resulting multi-materials, especially at the interfaces. Some AM technologies only allow the interchange (and bonding) of different materials between layers to lead to the generation of planar multi-material interfaces, while others can deliver and bond any materials throughout the build to achieve complex multi-material interfaces.

There are five AM technologies, according to the ASTM F2792−12a standard [54], that are suitable for the fabrication of metallic biomaterials, including powder bed fusion, directed energy deposition, sheet lamination, binder jetting, and material extrusion. Each of these AM technologies has its own capabilities and limitations, and may or may not meet the requirements for multi-material fabrication.

2.1. Powder bed fusion

Powder bed fusion works by delivering a layer of metal powder and then selectively melting or sintering the desired area by using laser or electron beam. The process iteratively continues by lowering the build plate, spreading another metal powder layer over the previous layer, and selectively melting or sintering this layer and the layer(s) beneath. Selective laser melting (SLM) is the most common powder bed fusion technology for fabricating metallic biomaterials. This technology usually utilizes only one powder bed dispensing system for one single metal powder, which makes the fabrication process challenging to accommodate the *in situ* delivery of multiple materials, unless a multi-material powder mixture is prepared beforehand. By using blended metal or metal-ceramic powder mixtures in the powder bed (Figure 2a), multi-material SLM has been applied for the multi-material fabrication of Ti-based [53–64] and Mg-based [67–70] biomaterials.

In situ multi-material SLM for Ti-based biomaterials enhanced the hardness and wear resistance through the *in situ* reinforcement of titanium with SiC [55], Si_3N_4 [56], TiB_2 [57,58], or hydroxyapatite (HA) [59,60]. In addition, the *in situ* SLM of titanium with Mo [61], Nb [62,63], and Ta [64], improved biomechanical compatibility with bone in terms of elastic modulus, in comparison with the elastic moduli of pure Ti and Ti-6Al-4V. Moreover, the *in situ* alloying of Ti-6Al-4V with Cu [65,66] has been shown to upregulate the angiogenesis-related genes and demonstrate antibacterial properties.

For Mg-based biomaterials, the *in situ* alloying of Mg with Zn during SLM [67] has been explored and the relationships between Mg-Zn composition, defects, and mechanical characteristics have been studied. In addition, pre-alloyed Mg-based biomaterials (*e.g.*, ZK60 and Mg-3Zn) have been *in situ* alloyed with rare earth elements (*e.g.*, Nd [68] and Dy [69]) during SLM, for improved corrosion resistance and prolonged biomaterials integrity. Furthermore, the *in situ* alloying of ZK60 with Cu [70] has been found to provide the base alloy with antibacterial properties and improved the compressive strength. Furthermore, for Fe-based biomaterials, SLM of pre-milled Fe and Mn powders enhanced the biodegradation rate and mechanical properties of the iron [71,72].

To obtain the intended multi-functionality for the biomaterials, optimum SLM processing parameters must be selected to allow for the sufficient diffusion of alloying elements into the base materials [55,56]. Tuning laser energy density, while avoiding the formation of undesirable internal pores and excessive melting, is challenging due to the distinctly different thermal properties of multiple materials. Some alloying elements have very high melting points and cannot be completely melted and diffused, and as a result partially melted material remains next to the matrix [62,64]. To bridge the gap in thermal properties, the particle size distributions of multi-material powders can be varied, with a higher melting point material having smaller particle sizes [63]. In addition, post-AM heat

treatment may be necessary to improve the multi-material diffusion and homogeneity in chemical composition [62]. Furthermore, the delivery of multi-material powders to the powder bed is an equally important aspect to ensure a uniform multi-material distribution within the resultant biomaterial [64]. Since powder bed fusion operates with high thermal energies, this AM process is also prone to high temperature gradients, which can cause cracks and distortions in the multi-material structure.

Using powder bed fusion for building *in situ* multi-functional AM metals or metal-ceramic composites requires complex and comprehensive process optimization to ensure proper selection of the laser power and the other process parameters that have to be aligned with the physical properties and powder characteristics of each of the materials. In addition, the steps required for the recycling and reuse of the leftover materials in the powder bed need to be considered.

2.2. Directed energy deposition

In directed energy deposition, a metallic material is delivered in the form of powder or wire through a nozzle, which is then melted by using thermal energy. Laser engineered net shaping (LENS) is the most common commercial process used for directed energy deposition. This technology offers a straightforward multi-material delivery system through multiple nozzles and the capability of *in situ* deposition and synthesis of different materials to obtain multi-material gradients in the structure (Figure 2b). In addition, compositionally graded structures can be produced by depositing one material and gradually replacing that material with another. Using multi-material LENS, Ti-based biomaterials have been *in situ* alloyed with boron [73,74] or reinforced with HA (under a N_2 atmosphere) [75], CaP [76], Nb-Zr-Ta elemental powders [77], and Zr-BN [78] to improve the hardness and wear resistance of the base biomaterial. Compositionally graded Co-Cr-Mo coating on Ti-6Al-4V

surface [79] and TiO_2 coating on Ti surface [80] have been fabricated to minimize the wear-induced loosening of metal-on-metal implants.

Similar to the laser-based multi-material AM processes based on powder bed fusion, the vast differences in the thermal properties of multiple materials have to be comprehensively investigated, in order to match these with the laser parameters and process parameters to create multi-functional structures with no structural or metallurgical defects. Despite the fact that directed energy deposition has the ability of *in situ* deposition of multiple materials, this AM process is less suitable for fabricating structures with fine geometries or hollow passages, which are often required for complex porous biomaterials designs [81]. Apart from that, this technology suffers from the common drawbacks of laser-based AM processes, i.e., high thermal gradients, which can induce residual stresses and metallurgical defects.

2.3. Sheet lamination

Sheet lamination is performed by stacking, bonding, and cutting foil materials into a 3D structure, after which an additional machining or milling process is required to make a specific structure. Ultrasonic consolidation is the most commonly used technique for bonding metallic foils [82–84]. Although the main advantages of this technology lie in the low operating temperature and the capability of producing large-scale structures at low costs, this technology has not yet been reported for the fabrication of multi-materials for bone substitutes.

Although sheet lamination accommodates simultaneous multiple foil feeding, due to the stacking and bonding of foils (Figure 2c), multi-material interfaces occur only in the planar direction. The major drawback of this technology concerns the voids occurring along the foil interfaces due to excessive and/or insufficient welding, surface roughness, or inaccuracy in the manual positioning of the foils. Such defects create a low bonding strength between the

layers and increase the possibility of delamination, which leads to poor mechanical properties of the resulting structure under shear and tensile loading. Considering the capabilities of this technology, the sheet lamination technology is more suitable for an embedded application, rather than multi-material AM for porous bone-substituting biomaterials, where mechanical integrity is one of the most important criteria.

2.4. Binder jetting

Binder jetting operates in a similar manner to powder bed fusion, but instead of applying thermal energy to fuse metal powder feedstock, an adhesive liquid is dispensed on the surface of the powder bed, bonding powder particles to form a desired structure. Since an adhesive liquid is delivered, the compatibility of the binder with metal powders, as well as the bonding properties are of great importance. Several types of adhesives are available, such as polymer binders, particle suspension inks, metallic salt compounds, and organometallic inks [85].

For multi-material binder jetting, a powder bed similar to the one required in powder bed fusion processes is utilized, meaning that this technology requires a carefully designed multi-material powder handling system for the preparation of blended multi-material powder prior to AM, as well as the systems for recycling and reusing the leftover powders after AM. Multi-material binder jetting with blended multi-material metal powders (Figure 3a) has been studied for porous Fe-Mn [86] and Fe-Mn-Ca [87] biomaterials to enhance the biodegradation rate of iron and to develop anti-ferromagnetic properties.

Porous binder-jetted biomaterials (*e.g.*, Fe-Mn [86] and Fe-Mn-Ca [87]) are composed of adhesive-bound powders. As such, post-AM debinding and sintering are needed to remove the binder and subsequently fuse multi-material powder particles together. Since the binder-jetted adhesive-bound porous structure is built inside a powder bed, it is required to remove loose powder particles from pores before post-AM heat-treatment, without damaging

the structural integrity of the biomaterial. If loose powder particles inside pores are not completely removed, they will fuse into the structure during sintering, compromising the interconnectivity of the pores and reducing the fidelity of the morphological properties of the final biomaterial. The as-printed structure is usually cured to strengthen the adhesive bonding [86], then high-pressure air is applied to remove loose powder particles before sintering [86].

Although removing loose particles in a green structure is demanding, there are no residual stresses created during the binder jetting process, due to the absence of direct laser heating and rapid cooling during fabrication. However, post-AM sintering causes structural shrinkage, as a consequence of binder decomposition and powder particle rearrangement and integration. As an example, Fe-Mn-Ca biomaterials shrank about 11.7% in all directions [87]. In summary, the application of binder jetting for the fabrication of multi-functional porous AM metals or metal-ceramic composite biomaterials not only requires intricate multi-material powder handling systems before and after AM, but also necessitates some steps to remove loose powder particles from the adhesive-bound porous structure and to sinter the particles through a subsequent post-AM heat treatment.

2.5. Material extrusion

Extrusion-based AM technology works by continuously pushing metal or ceramic powder-based feedstock through a nozzle or nozzles to build a 3D structure layer by layer. The feedstock materials should have viscoelastic properties that enable them to flow through the nozzle, solidify immediately upon extrusion, and maintain the shape even when they are stretched over the space of the underlying layers [88]. The feedstock materials can be designed to comprise powdered materials of various compositions mixed with a polymer binder. The compatibility of the feedstock material with the binder should avoid undesired interactions during mixing, extrusion, debinding, and even sintering. For multi-material AM

purposes, more than one nozzle can be integrated to deliver different feedstock materials and achieve complex multi-material interfaces within the structure. Alternatively, one feedstock of multi-material can be prepared and delivered through one single nozzle.

Material extrusion with blended multi-material powder-based feedstock (Figure 3b) has been pursued [89–91], since it has no drawbacks inherent to the laser-based AM technologies that were described earlier, such as residual stresses, cracks, distortions, and even metallurgical defects. Using this technique, Fe-based biomaterials (*e.g.*, Fe-$CaSiO_3$) has been realized for bone cancer treatment as well as for regenerating cortical bone defects [89]. The extruded Fe-$CaSiO_3$ composite is composed of an adhesive-bound multi-material powder mixture, which requires post-AM debinding and sintering. Since the adhesive-bound structure is not built in the powder bed, it saves the powder handling steps of recycling and reusing multi-material powder, as well as the post-AM step to remove loose powder particles.

The main limitation of this technology lies in the printing resolution, which is strongly dependent on the powder particle size and the nozzle diameter. In addition, building a part with a large aspect ratio and an overhanging structure can only be achieved by controlling the composition of the feedstock and its rheological properties in order to ensure consistent flow and fast solidification. Designing suitable multi-material feedstock is the most crucial step to achieve complex structures with multi-material interfaces.

2.6. Selection of multi-material AM technologies for the fabrication of multi-functional metallic bone substitutes

Choosing a suitable multi-material AM technology for fabricating multi-functional porous metallic biomaterials requires a comprehensive knowledge of the capabilities and limitations of each of the processes described earlier. The basic requirements for a multi-material AM technology concern the capabilities of delivering multiple materials,

achieving complex multi-material interfaces, and ensuring strong bonding between the materials of different types and compositions.

With respect to the material delivery systems that influence the multi-material interaction, three systems have been implemented in AM technologies, namely powder bed dispensers, nozzles, and foil material delivery systems. The AM processes based on powder bed fusion, binder jetting, directed energy deposition, and material extrusion allow for the building of complex multi-material interfaces, while sheet lamination can only create planar multi-material interfaces.

Moreover, the cost effectiveness in relation to the material delivery system is another issue to address. Using a powder bed dispensing system to build complex multi-material interfaces requires an advanced powder handling system to allow for the recycling and reuse of multi-material powder mixtures. A post-AM step is needed to remove the unbound or unmolten powder particles entrapped in the pores of structures. This step is demanding, especially for binder jetting, as the as-built structure is bound only by an adhesive material and is, thus, vulnerable. Multi-material deposition using nozzles in material extrusion and directed energy deposition processes is capable of controlling the quantity of the materials needed, while recycling and reusing the powder or a post-AM step of removing loose powder particles are not required. Nozzles are, therefore, a more suitable material delivery means for multi-material AM.

In addition to the material delivery system, bonding between multiple materials is of critical importance for the performance of multi-functional porous AM metallic biomaterials. Two material bonding approaches are usually used in multi-material AM technologies including direct heating by laser or adhesive bonding by using a binder, followed by post-AM heat treatment. The chosen type of bonding also determines the final microstructure of the multi-material. Using direct heating in powder bed fusion and directed energy deposition

processes enables the *in situ* AM of multi-materials. This approach, however, requires advanced process control and management, due to the integration of laser energy into the AM machine and the vast differences in thermal properties between multiple materials. Adhesive bonding in binder jetting and material extrusion, on the other hand, is only capable of the *ex situ* AM of multi-materials and requires post-AM debinding and sintering. The biocompatibility of the residual binder entrapped inside the multi-material structure may be an important issue to consider.

AM using direct heating usually produces mechanically stable structures. However, there is a risk of having high thermal gradients and metallurgical mismatch, which may induce residual stresses or structural defects. Furthermore, this is a challenging approach for fabricating metals with low boiling points and high vapor pressures. On the other hand, the post-processing of adhesive-bound AM structures is usually conducted in a homogenously heated furnace, which allows the materials to diffuse slowly and bond strongly through sintering. Although sintering leads to the shrinkage of the structure, this can be compensated for during the design phase and minimized during fabrication. In addition, the parameters of the sintering processing can be optimized to yield high-density structures, which presents an opportunity to fabricate not only porous but also fully dense biomaterials for bone substitutes. Based on the advantages and disadvantages of each of bonding approaches, adhesive bonding followed by sintering seems to be a better choice for multi-material bonding.

Comparing the five available multi-material AM technologies, material extrusion appears to be the most straightforward option for multi-material fabrication of multi-functional bone substituting biomaterials [89]. Material extrusion is capable of building multi-material interfaces. Moreover, material extrusion does not directly heat the feedstock materials to fuse the multiple materials, making it less probable to create metallurgical defects in the structure. In addition to Fe-$CaSiO_3$ scaffolds that were aimed for bone

substitutes [89], multi-material extrusion AM has been applied to fabricate materials for other types of application including hydroxyapatite-based surgical biomaterials, graphene-based materials for biomedical electronic devices, and other multi-element materials systems such as Fe-Ni-Cr, Al-Mg-Cr-Fe and Ag-Cu for various applications [90–94].

3. BIOMATERIALS FOR MULTI-FUNCTIONAL METALLIC BONE SUBSTITUTES

An ideal metallic biomaterial for bone substitutes should not only be biocompatible and fulfill the design requirements in geometry, but also have mechanical and biological functionalities that are needed for bone replacement and regeneration. In the case of the bone substitutes aimed for permanent load-bearing applications, long-term mechanical properties, corrosion resistance, and osseointegration are the most important factors to consider. However, for temporary bone repair applications, biodegradability, short-term mechanical integrity, and biological functionalities for osteosynthesis are the critical considerations.

For bone substitutes to achieve multiple functionalities, more than one material is often needed. The concept of multi-material synthesis and processing for improved physical characteristics, chemistry, and mechanical performance, which may be achieved through powder metallurgy, and for enhanced biological performance such as cell attachment through surface modification, has been established long before the development of multi-material AM technologies. Therefore, developing multi-material compositions specifically suitable for AM technologies requires multi-disciplinary knowledge about the intrinsic properties of each of the materials and the understanding of the interactions between different materials in order to meet the functional requirements of the synthesized biomaterials aimed to be used as bone substitutes.

In this section, recent progress in developing Ti-, Mg-, and Fe-based biomaterials for bone substitutes, including advances in (multi-material) AM technologies applied for the development of permanent or temporary bone replacements, is reviewed.

3.1 Ti-based biomaterials

Titanium and its alloys are promising biomaterials for permanent bone replacement due to their biocompatibility, lightweight, high strength, and superior corrosion resistance. To be able to use them as long-term bone replacements, titanium and its alloys should possess bone-mimicking mechanical properties, which can be obtained through the optimization of the geometry of the porous structure and realized using AM technologies (Figure 4a) [95–101]. Porous Ti-based bone substitutes also improve osseointegration and can be made patient-specific (Figure 4b) [102], which is essential for preventing implant failure due to inadequate integration of the implant into the surrounding bony environment.

In craniofacial and orthopedic applications, patient-specific AM Ti-based implants have shown remarkable improvements over other alternatives, since they are fabricated to fit precisely into bony defects. This is beneficial, since it reduces the probability of implant failure due to loosening. In a six-month follow-up of a custom-designed AM titanium implant for a large skull defect, no complications were observed [103]. In addition, a clinical study on 21 patients with custom-made AM Ti-6Al-4V implants during a follow-up of 6 to 24 months demonstrated osseointegration and skull symmetry [104]. For orthopedic applications, patient-specific AM titanium implants were reported to be effective with no complications, when replacing distal tibia bone defects with multiple fractures in the foot and talus [105]. Furthermore, a success rate of 86.7% has been reported in a 22 month follow-up study on 15 patients treated with patient-specific AM titanium implants for foot ankle deformity corrections and arthrodesis procedures [106]. Overall, AM patient-specific designs improved the mechanical stability of Ti-based implants.

Surface biofunctionalization of AM porous Ti-based biomaterials have been performed to improve their bioactivity and induce antibacterial properties to prevent implant-associated infections. The integration of Ca and P elements and immobilized Ag nanoparticles into the

surface of porous AM Ti-6Al-4V implants (Figure 4c) has been demonstrated to afford AM biomaterials with antibacterial properties against methicillin-resistant *Staphylococcus aureus* (MRSA), while stimulating the growth of human MSCs [38]. Moreover, the surface bioactivity of AM porous Ti-6Al-4V biomaterials has been shown to be enhanced with the incorporation of Sr, which induces more bone formation and stimulates bony ingrowth [107].

While pure titanium and Ti-6Al-4V dominate the research on Ti-based AM biomaterials, *in situ* multi-material AM of Ti-based biomaterials using the powder bed fusion [53–64] and directed energy deposition [73–80] techniques have led to improved properties and functionalities, including improved hardness and wear resistance, lower values of elastic modulus, tunable fracture toughness, and enhanced biocompatibility. These improvements have been achieved through phase changes, grain refinement, precipitation of second phases, and reinforcement by a second component.

The *in situ* SLM of Ti powders with SiC (in a molar ratio of 8:3) and Si_3N_4 (in a molar ratio of 9:1) has been reported to result in viable TiC-Ti_5Si_3 and TiN-Ti_5Si_3 composites [55,56]. During the process, both TiC and TiN phases were formed through a dissolution/precipitation mechanism and subsequent grain growth [55,56]. The TiC phase reached the most refined dendritic morphology and a dendritic trunk length of 4.5 µm, at a laser power of 80 W and a scanning speed of 0.2 m/s (Figure 5a) [55]. The TiN phase exhibited an optimum refined near-round morphology at a laser energy density of 5 kJ/m and a scanning speed of 0.2 m/s [56]. As a result of the grain refinement strengthening, the TiC-Ti_5S_3 composites achieved a lower friction coefficient of 0.2 as compared to pure Ti (~1.3) and a microhardness value of 980.3 HV, which is three times higher than that of pure Ti [55]. Similarly, the TiN-Ti_5S_3 composites had an improved, uniform wear rate of 6.84×10^{-5} mm^3/Nm with a low friction coefficient of 0.19 [56].

Moreover, the fine eutectic TiB grains formed through the *in situ* dissolution of Ti and B and subsequent precipitation were distributed along the Ti grain boundaries (Figure 5b). The *in situ* LENS Ti-TiB composites made of pure Ti and 1.6 wt.% B powders enabled the design of a quasi-continuous network microstructure when fabricated with 200 W laser power [73]. The homogenous microstructure of the Ti-TiB composites led to a greater hardness value of 392.6 HV and better wear resistance with a wear rate of 2.4×10^{-3} mm^3/Nm as compared to those of pure Ti (345.5 HV and 6.1×10^{-3} mm^3/Nm, respectively) [74]. In addition, the *in situ* SLM of Ti-6Al-4V with 3 wt.% TiB_2 powders fabricated using a laser power of 240 W created needle-like TiB grains of 0.5 to 1 µm in size. The Ti-6Al-4V-TiB composites possessed two times higher wear resistance compared with the Ti-6Al-4V alloy [57].

A series of *in situ* SLM trials to reinforce pure titanium with 2 − 5 wt.% HA (nano-sized) under different process conditions resulted in varied microstructures (Figure 5c) and improved microhardness and nanohardness values [59]. However, the fracture toughness of the composites decreased from 3.41 MPa $m^{1/2}$ to 0.88 MPa $m^{1/2}$ as the HA content increased [60]. The reduced toughness was due to the formation of the fragile $CaTiO_3$ and Ti_5P_3 phases that are susceptible to crack initiation and propagation. Nevertheless, the toughness of the Ti-HA composites was still in the range of those reported for the native trabecular bone. Additionally, the *in situ* LENS of Ti-6Al-4V with 5 wt.% HA [75] and pure Ti with 10 wt.% CaP [76] resulted in significant (*i.e.*, up to 95%) improvements in wear resistance. In *in situ* Ti-6Al-4V-HA and Ti-CaP composites, the $CaTiO_3$ and $Ca_3(PO_4)_3$ phases were developed, which formed a tribological layer protecting the biomaterial surface [75,76].

Apart from hardness and wear resistance, the *in situ* formation of β-phase Ti alloys (Figure 5d) is also desired to improve the match between the elastic moduli of Ti-based

biomaterials and the bone. *In situ* SLM using blended elemental powders of Ti-6Al-4V-10Mo [61], Ti-40.5Nb [63], Ti-35Nb [62] and Ti-50Ta [64] (in wt.%) have been shown to result in significantly decreased elastic moduli ranging between 73 and 84.7 GPa as compared with α-phase pure Ti or dual-phase Ti-6Al-4V (105 − 120 GPa). In addition, the β-phase Ti alloy (Ti-35Nb-7Zr-5Ta) fabricated through *in situ* LENS of elemental powders has been found to demonstrate a higher trans-passive potential of > 5 V, confirming its superior corrosion resistance when compared to pure titanium (*i.e.*, ~1.5 V) [77]. A higher trans-passive potential can be attributed to higher adherent oxides including not only TiO_2 but also Nb_2O_5, Ta_2O_5, and ZrO_2 that are developed on the alloy surface as the alloy is corroded [77].

Regarding the biological performance, *in situ* SLM Ti-6Al-4V-Cu made from Ti-6Al-4V and 6 wt.% Cu powders not only maintained a high *in vitro* proliferation rate and alkaline phosphatase (ALP) activity (Figure 6a-b), but also controlled the inflammatory responses [66]. Macrophages were found to be less active on the surfaces containing Cu and the pro-inflammatory cytokine of IL-6 was significantly suppressed (Figure 6c-d) [66]. Furthermore, *in situ* Ti-6Al-4V-6Cu allowed the proliferation of human umbilical vein cells (HUVECs) and remarkably upmodulated the angiogenesis-related gene expressions of VEGF-A (Figure 6e-f) [66]. The inclusion of 6 wt.% Cu also demonstrated antibacterial properties against *E. coli* and *S. aureus* (Figure 6g-h) [65].

AM Ti-based alloys have displayed a promise for the treatment of critical bone defects. The state-of-the-art *in situ* multi-material AM using powder bed fusion and directed energy deposition has demonstrated the ability to develop multi-functional Ti-based biomaterials. Most of the abovementioned studies on multi-material AM Ti-based materials were focused on the improvements in microstructure and mechanical characteristics, leaving a large scope for validation in terms of biocompatibility. Further research should be conducted to clarify

the achievable multi-functionalities that also include the biocompatibility of additional alloying elements and the constituents that are formed in the multi-material Ti environment.

3.2 Mg-based biomaterials

Magnesium and its alloys have been extensively studied for temporary bone fixation devices and have been reported to have a great potential for applications in low load-bearing bone substitution [108]. The elastic modulus of magnesium is relatively low, which aids in preventing mechanical failure due to stress shielding. Moreover, the biodegradability of Mg provides it with a unique potential for temporary bone replacement.

Mg-based biomaterials are expected to maintain mechanical integrity at the early stage of bone healing and to be eventually replaced by *de novo* bone tissue [109]. Magnesium degrades rapidly and releases hydrogen, which can be problematic. For example, excessive hydrogen gas creates mechanical interferences during bone healing. Additionally, the diffusion of hydrogen into subcutaneous tissue can lead to imbalance in blood parameters [110], which is why the biodegradation rate of Mg should be controlled.

Surface biofunctionalization of bulk Mg alloys has been performed to improve their mechanical integrity during biodegradation and to enhance their biocompatibility [109]. Coating Mg alloys with Ca-P [111,112], and Si [113] provides these alloys with protective layers that reduce their corrosion rates and prevent significant mechanical losses at an early stage. These surface modifications also contribute to enhancing bone growth during biodegradation. Another approach to controlling the biodegradation rate of Mg-based biomaterials is to alloy Mg with rare earth (RE) elements. The addition of RE elements, such as Dy [114], Gd [115], Nd [116], and Y [117,118] to magnesium through conventional powder metallurgy methods has been commonly used to improve its corrosion resistance.

An *in vivo* study, comparing fast and slowly degrading Mg-based biomaterials of ZX50 and WZ21 (Figure 7a), was performed on rat femurs for up to 36 weeks to evaluate their

biodegradation profiles and biocompatibility [118]. ZX50 that contained no RE elements had a rapid biodegradation profile. The deterioration of the mechanical integrity occurred in the first week and complete biodegradation occurred in 16 weeks. As a consequence, bone healing was disturbed due to massive hydrogen release (*i.e.*, ~270 mm^3 daily) [118]. In contrast, WZ21 that contained the rare earth element Y could maintain its mechanical integrity for up to 4 weeks. The daily release of approximately 130 mm^3 hydrogen gas did not interrupt the bone healing process. Enhanced bone formation was observed on the surface of WZ21 specimens, implying the osteogenic properties of the biomaterial. When compared to ZX50, WZ21 was able to combine both good mechanical integrity and biocompatibility with an appropriate corrosion rate suitable for bone regeneration [118].

The developments of Mg-based biomaterials with a controlled biodegradation profile and bone-mimicking mechanical properties have encouraged surgeons to consider the prospects of biodegradable implants for clinical applications. Currently, there are three Mg-based bone screws available in the market made from the alloys Mg-Y-RE-Zr [119] and Mg-Ca-Zn [120] as well as pure Mg [121].

Clinical trials on bone screws made from the Mg-Y-RE-Zr alloy have shown therapeutic results that are comparable to titanium screws in terms of the American Orthopedic Foot and Ankle Score (AOFAS) for hallux, the range of motion for the metatarsophalangeal joint, and pain assessment for hallux valgus osteotomies [119]. In addition, the screws made from Mg-Y-RE-Zr showed high degrees of osseointegration after 6 months, with no revision surgeries required. In a different study, Mg-Ca-Zn screws successfully fixed the distal radius fractures of 53 patients [120]. Acceleration of bone healing was reported due to the accumulation of Ca on the screws during biodegradation. Complete bone regeneration was achieved within one year along with the biodegradation of entire screws (Figure 7b). Furthermore, pure Mg screws were utilized for the treatment of

23 patients with osteonecrosis in the femoral head [121]. The Mg screws demonstrated good fixation during biodegradation and promoted osteogenesis.

Despite the positive clinical progress of bulk Mg screws, the utilization of the AM technology for magnesium alloys is challenging due to the intrinsic properties of magnesium that has a high oxygen affinity, a low boiling point, and a high vapor pressure. Indeed, there is only one comprehensive study on the *in vitro* biodegradation behavior and the evolution of the mechanical properties of the laser-based AM porous WE43 magnesium alloy during *in vitro* biodegradation [29]. The porous AM WE43 Mg alloy, fabricated using SLM, was designed to have a topologically ordered open-cell structure for enhanced interactions with the surrounding cells and tissue. The AM WE43 Mg alloy was able to preserve ~80% of its volume (Figure 8a) and maintain its mechanical properties at a level of the mechanical properties of trabecular bone for up to four weeks of *in vitro* biodegradation in a revised simulated body fluid (Figure 8b-c) [29].

Utilizing adhesive-based AM processes for Mg-based biomaterials is challenging as well, as the polymer binder and solvent constituents have to be compatible with magnesium. Recent developments of solvent capillary-driven techniques using binder jetting have helped in minimizing the metallurgical complexities involved in the AM of Mg alloys [122]. The framework involves only a solvent to interact with the outermost layer of magnesium powder particles (*i.e.*, MgO), forming a strong interparticle capillary-bond that assembles powder particles into a 3D structure (Figure 8d-e). In the absence of polymer, prior to post-AM sintering, a debinding step is not required and the solvent will decompose during the sintering process. The AM process utilizing the binderless capillary-bond approach has been shown to result in a Mg-Zn-Zr alloy with 1.3 g/cm^3 density, 27% apparent porosity, and 18.4 GPa of elastic modulus mimicking the human cortical bone (Figure 8f) [123].

In addition, several studies on *in situ* multi-material AM of Mg-based biomaterials have been conducted using the SLM technology with blended powders to achieve high relative density Mg alloys, controlled biodegradation rates, improved strengths, and antibacterial properties. *In situ* AM of binary Mg-Zn alloys with variations in the composition of the Zn powder was performed to understand the mechanical characteristics of the resulting materials [67]. Interestingly, only the Mg-1Zn alloy could reach a high relative density of 99.35% with almost no defects. As the Zn content increased from 2 to 12 wt.%, the Mg-Zn alloys suffered from solidification cracking due to the presence of solidification shrinkage stresses that tore the liquid films composed of eutectic liquid phases. Among the *in situ* SLM binary Mg-Zn alloys (Figure 9a), the Mg-1Zn alloy exhibited the best mechanical properties with a hardness value of 50 HV, an ultimate tensile strength of 148 MPa, and an elongation value of 11%, which were similar to those of cast Mg-1Zn counterparts [67].

Furthermore, a series of *in situ* SLM experiments with pre-alloyed ZK60 added with 1.8 − 5.4 wt.% rare earth Nd powder demonstrated an optimum biodegradation rate of 1.56 mm/year, with the *in situ* formed alloy containing 3.6 wt.% Nd [68]. The enhanced corrosion resistance of the ZK60-3.6Nd alloy was attributed to the formation of fine Mg-Zn-Nd intermetallic phases along the α-Mg grain boundaries (Figure 9b), which created tight junctions that prevented the propagation of corrosion. With a higher Nd concentration (*i.e.*, 5.4 wt.%), however, more Mg-Zn-Nd intermetallic phases were formed and more sites of galvanic corrosion occurred, which counteracted the beneficial effects from grain refinement and increased the corrosion rate [68]. In another research, the *in situ* addition of 0.4 wt.% Cu to ZK60 during SLM resulted in a ZK60-0.4Cu alloy whose degradation rate was similar to ZK60, (*i.e.*, 1.01 mm/year) but exhibited antibacterial properties as well (Figure 9c-d) [70]. The addition of Cu also resulted in an enhanced compressive strength up

to 158.3 ± 5.1 MPa, due to uniformly distributed Mg-Zn-Cu phases and grain refinement strengthening.

In conclusion, several studies focusing on the biodegradable behavior and mechanical integrity of Mg-based biomaterials have been performed. The clinical trials of Mg-based bone screws have shifted the paradigm of corrosion resistance towards a new perspective of temporary bone fixation implants. Following the positive outcomes, the research on (multi-material) AM technologies for Mg-based biomaterials is now advancing. Even though a few research groups have successfully produced (multi-material) AM Mg alloys [67–70], more studies are required to better understand and control the AM processes and the biodegradation profiles, mechanical integrity, and biocompatibility of these materials.

3.3 Fe-based biomaterials

Iron and its alloys have been studied for temporary load-bearing bone replacements. They combine biodegradable behavior with high mechanical strength and ductility [124]. As compared to Mg-based materials, Fe-based biomaterials have the advantage of not releasing hydrogen as they degrade. Their biodegradation products, being not completely dissolvable in physiological solutions, have been found to hinder the release of iron ions and slow down the biodegradation process [125]. In addition, the ferromagnetic nature of iron may need to be altered prior to using it for the fabrication of imaging-friendly implantable devices.

Various methods including alloying with Mn or noble metals and reinforcing with bioceramics through powder metallurgy techniques have been investigated to accelerate the biodegradation rate and reduce the magnetic properties of iron [125]. Among the alloying elements, manganese is considered promising, since it can not only improve the biodegradation rate of iron [126–128], but can also lead to anti-ferromagnetic Fe-Mn alloys [129]. A trace of manganese has been found to play an important role in osteogenesis and bone resorption [130]. Besides manganese, noble metals, such as Ag, Au, Pd, and

Pt [131–133] have been used to create second phases in Fe-based alloys (*e.g.*, Fe-Ag, Fe-Au, Fe-Pd and Fe-Pt), which can induce micro-galvanic coupling to stimulate Fe degradation.

Even though alloying pure iron can speed up its biodegradation in *in vitro* tests, such improvements have not been observed *in vivo*. The non-invasive monitoring of pure iron and iron reinforced with 5 wt.% bioceramics (*i.e.*, HA), tricalcium phosphate (TCP), or biphasic calcium phosphate (BCP) implanted in sheep forelegs for 60 days has shown insignificant reductions in the sizes of these biomaterials [134,135]. Similarly, two Fe-based alloys, namely Fe-10Mn-1Pd and Fe-21Mn-0.7C-1Pd (in wt.%), have displayed almost no structural changes after implantation in rat femurs for 52 weeks (Figure 10a) [136]. Although signs of degradation were present, no remarkable weight reductions were observed (Figure 10b). The inadequate biodegradation rate was explained by insufficient oxygen transport to the biomaterial surface, due to a dense layer of biodegradation products that wrapped around the surface and hindered further degradation of iron [136]. These findings suggest that Fe-based biomaterials should be designed to be highly porous so as to allow high permeability for accelerated biodegradation.

As for biocompatibility, *in vivo* studies on bulk Fe-based biomaterials have reported no systemic toxicity [124]. The Fe-10Mn-1Pd and Fe-21Mn-0.7C-1Pd alloys were found to show no signs of local toxicity or clinical abnormalities, when implanted transcortically in 38 rat femurs for 52 weeks [136]. Although Fe ions were present in the biomaterial's vicinity (Figure 10c), no harm to the neighboring bone tissue was observed. The Fe-based biomaterials were well integrated and enveloped by a narrow flap of connective tissue. In addition, an *in vivo* study on pure iron and Fe-bioceramic composites including Fe-5HA, Fe-5TCP, and Fe-5BCP, have exhibited no systemic toxicity after 60 days of implantation in sheep forelegs [134]. Normal dynamic blood responses and no cellular stresses were observed throughout the *in vivo* study. Histological analysis determined the presence of

inflammatory cells (*i.e.*, macrophages, granular tissue, and fibrous tissue) surrounding the Fe-bioceramic composites, as the sign of active biodegradation and wound healing process (Figure 10d) [134].

On the other hand, an *in vivo* study on Fe-30 wt.% Mn implanted in rat femurs reported that the biomaterial might act as a local irritant, although the finding was not statistically significant [137]. A small-scale necrotic bone was found to be engulfed in the corrosion products along with the presence of macrophages. Nonetheless, there were no adverse systemic effects determined [137]. Furthermore, the addition of silicon to Fe-Mn biomaterials has been found to improve their biocompatibility. In an *in vivo* study of a bulk Fe-Mn-Si alloy (with a ratio of 3:2:2) implanted in rat tibia for 28 days, the bone regeneration process was found to continue [138]. An increase in the ALP activity after 14 days of implantation suggested active bone formation. Moreover, histological analysis confirmed the start of bone remodeling after two weeks, when some apoptotic osteocytes were observed, followed by the appearance of osteoblasts at week 4 (Figure 10e) [138]. Overall, a normal blood homeostasis was observed during the slow biodegradation of the Fe-Mn-Si alloy.

Recent developments of AM technologies have opened up new possibilities to improve the biodegradation profiles of Fe-based biomaterials through porous topological and multi-material designs. *Ex situ* binder-jetting of Fe-30 wt.% Mn with an open porosity of 36.3% has been shown to result in a material with an electrochemical corrosion rate of 0.73 mm/year, which is ~11 times higher than that of pure iron with the same exposed surface area [86]. Moreover, the inclusion of 1 wt.% calcium in the pre-alloyed binder-jetting of Fe-35 wt.% Mn increased the biodegradation rate from 0.04 mm/year to 0.07 mm/year (Figure 11a-b) [87]. Furthermore, AM topologically ordered porous pure iron with 80% porosity has demonstrated an electrochemical corrosion rate of 1.18 mm/year, which is

~12 times higher than that of cold-rolled iron, and has led to a lower impedance value as compared to its cold-rolled counterparts (Figure 11c-e) [30].

Although the electrochemical corrosion values of AM porous Fe-based biomaterials have been generally found to increase, validation through *in vitro* immersion tests is still required. After 4 weeks of static immersion in a revised simulated body fluid, porous AM pure iron achieved only 3.1% weight loss [30]. The small mass reduction was attributed to the dense corrosion products that covered the porous structure (Figure 11f), preventing further biodegradation of porous iron from occurring. Similarly, *in vitro* immersion of binder-jetted Fe-30Mn resulted in a negligible weight loss [71,86]. These outcomes may also be due to an inadequate *in vitro* fluid flow, different atmosphere conditions from those occur *in vivo*, as well as the absence of blood cells and macrophages, which could have contributed to the faster biodegradation of biomaterials and the removal of the corrosion products. Obviously, performing a long-term *in vivo* biodegradation study on porous AM Fe-based biomaterials is of critical importance. However, no such studies have been performed to date. Recently, a 4-week *in vivo* study of SLM Fe-35 wt.% Mn, having a 43% porosity, has shown an on-going new bone forming process with good bony-implant integration [71].

In addition to an improved rate of electrochemical biodegradation, the progress in AM using multi-material has introduced other functionalities to Fe-based biomaterials including anti-ferromagnetic properties, improved osteosynthesis properties, and assistance in cortical bone cancer treatment. *Ex situ* binder-jetted Fe-30Mn [86] and Fe-35Mn-1Ca [87] have been shown to generate ε-martensite and γ-austenite Fe-Mn phases (Figure 12a-b) during the post-AM sintering stage. The ε and γ-Fe-Mn phases possessed the intrinsic anti-ferromagnetic properties [139]. Furthermore, *ex situ* Fe-30$CaSiO_3$ (in wt.%) composites fabricated using material extrusion not only improved the *in vivo* osteosynthesis significantly as compared to pure iron but also demonstrated the potential for bone cancer therapy

(Figure 12c). In the case of a Fe-30$CaSiO_3$ biomaterial synergized with laser and reactive oxygen species (ROS), the therapeutic effects of tumor treatment (Figure 12d) were enhanced, as demonstrated in an *in vivo* study [89].

Overall, Fe-based biomaterials have shown their potential as temporary load-bearing bone implants. Regardless of the systemic biocompatibility reported in all *in vivo* studies, Fe-based biomaterials may act as a local irritant, due to the toxicity of the corrosion products. Details on the interactions of Fe-based degradation products with bone tissue and inflammatory responses are still unclear. More research employing (multi-material) AM technologies for porous Fe-based biomaterials is required not only to improve the biodegradation profile, but also to understand the degradation behavior that strongly affects the biocompatibility of Fe-based biomaterials.

4. CONCLUDING REMARKS AND FUTURE PERSPECTIVES

The initial efforts of the bone tissue engineering community were mainly focused on fabricating biomaterials that mimic the macrostructure of the natural bone. Recent efforts have been mobilized to produce biomaterials using the AM technologies that allow for the realization of micro-architectured porous geometries and the placement of the right biomaterial at the right place for bone regeneration. Given the possibility of high-precision manufacturing of complex macro- and micro-architectured porous biomaterials, the AM technologies are undoubtedly linked to the future of metallic biomaterials for bone implants.

Clearly, AM technologies intrinsically provide the potential for multi-material fabrication that have not yet been extensively explored for bone implant applications. Using multi-material AM technologies, the functional requirements of biomaterials for bone implants, such as long-term mechanical properties for permanent use, short-term mechanical integrity, and biodegradation for temporary replacements, as well as biocompatibility, can be

tailored not only through structural design but also via adjustment of material types or compositions.

Among the available multi-material AM technologies, extrusion-based AM, using multi-material powder-based feedstock, appears to be the most straightforward option due to its capability of fabricating complex multi-material interfaces with a simple manufacturing process. For the multi-material extrusion-based AM to be successful in fabricating metallic bone substitutes, the fabrication processes, implant design, and material choice need to be properly selected. Understanding the chemistry of multiple materials in the feedstock, which may or may not affect the AM process, structure, and material properties, is essential. In addition, ensuring a homogenous distribution of multiple materials in the feedstock prior to AM and in the fabricated biomaterials is equally important in order to achieve near-isotropic material properties. Together with appropriate AM processing parameters, the multi-material feedstock with shear-thinning behavior and free-standing characteristics should allow continuous, stable deposition of structures even when the aspect ratios are high. Post-AM debinding and sintering need to be adjusted with respect to temperature, time, and atmosphere in order to achieve specific microstructures and biomaterial functionalities. Even though the multi-material extrusion-based technology has been so far primarily applied to Fe-based bone-substituting [89], it can, in principle, be applied to a wide range of powdered feedstock materials for various multi-functionalities, including metallic biomaterials, such as tantalum-based alloys and shape memory-based alloys

The future research on the multi-material extrusion-based AM for metallic biomaterials should be directed towards enhanced abilities to introduce materials of different types or compositions locally at a few micrometer scale within the structure. This will advance the technology towards improved control over the resulting implant properties. Additionally, fabricating geometrically complex multi-functional biomaterials should involve easily

dissolvable or decomposable sacrificial support materials that will pose no adverse effects on the performance and biocompatibility of the resultant biomaterials. Finally, combining multi-material extrusion-based AM with two-dimensional nanopatterning on each layer [140–142] during the fabrication process could further improve the functionalities of the final biomaterials through the optimization of surface nanotopography. Overall, multi-material extrusion-based AM technologies hold a great promise for advancing the state of the art in the fabrication of metallic multi-functional bone substitutes.

In short, substantial progress has been made in developing multi-functional Ti-, Mg-, and Fe-based biomaterials aimed for applications as orthopedic implants. AM Ti-based implants have been applied clinically, while the research is continuing on Mg- and Fe-based biomaterials. Multi-material AM of Ti-based biomaterials including alloys other than Ti-6Al-4V promises significant improvements in the microstructure, mechanical characteristics, and biological performance of the resulting materials including antibacterial properties, anti-inflammatory responses, and the upregulation of angiogenesis-related genes. For Mg-based biomaterials, multi-material AM has addressed the issue of decreasing the biodegradation rate of these alloys, while improving their mechanical strength and inducing antibacterial properties. Multi-material AM for Fe-based biomaterials aims at achieving faster biodegradation rates, altering the ferromagnetic properties of such materials and enhancing their biocompatibility. In conclusion, multi-material AM technologies are expected to enable the proper selection of materials and compositions to improve the functionalities of Ti-, Mg-, and Fe-based bone substitutes.

ACKNOWLEDGEMENTS

This work is part of the 3DMED project that has received the funding from the Interreg 2 Seas programme 2014 – 2020, co-funded by the European Regional Development Fund under subsidy contract No. 2S04-014.

5. REFERENCES

[1] J. Scheinpflug, M. Pfeiffenberger, A. Damerau, F. Schwarz, M. Textor, A. Lang, F. Schulze, Journey into bone models: A review, Genes (Basel). 9 (2018). https://doi.org/10.3390/genes9050247.

[2] B.Q. Le, V. Nurcombe, S.M.K. Cool, C.A. van Blitterswijk, J. de Boer, V.L.S. LaPointe, The components of bone and what they can teach us about regeneration, Materials (Basel). 11 (2017) 1–16. https://doi.org/10.3390/ma11010014.

[3] T.M. Keaveny, W.C. Hayes, Mechanical properties of cortical and trabecular bone, Bone. 7 (1993) 285–344.

[4] R. Florencio-silva, G. Rodrigues, E. Sasso-cerri, M.J. Simões, P.S. Cerri, B. Cells, Biology of bone tissue: Structure, function, and factors that influence bone cells, Biomed Res. Int. 2015 (2015) 1–17. https://doi.org/10.1155/2015/421746.

[5] G.M. Calori, E. Mazza, M. Colombo, C. Ripamonti, The use of bone-graft substitutes in large bone defects: Any specific needs?, Injury. 42 (2011) S56–S63. https://doi.org/10.1016/j.injury.2011.06.011.

[6] E. Roddy, M.R. DeBaun, A. Daoud-Gray, Y.P. Yang, M.J. Gardner, Treatment of critical-sized bone defects: clinical and tissue engineering perspectives, Eur. J. Orthop. Surg. Traumatol. 28 (2018) 351–362. https://doi.org/10.1007/s00590-017-2063-0.

[7] K.S. Griffin, K.M. Davis, T.O. McKinley, J.O. Anglen, T.M.G. Chu, J.D. Boerckel, M.A. Kacena, Evolution of bone grafting: Bone grafts and tissue engineering strategies for vascularized bone regeneration, Clin. Rev. Bone Miner. Metab. 13 (2015) 232–244. https://doi.org/10.1007/s12018-015-9194-9.

[8] T. Burk, J. Del Valle, R.A. Finn, C. Phillips, Maximum quantity of bone available for harvest from the anterior iliac crest, posterior iliac crest, and proximal tibia using a standardized surgical approach: A cadaveric study, J. Oral Maxillofac. Surg. 74 (2016) 2532–2548. https://doi.org/10.1016/j.joms.2016.06.191.

[9] J.K. McEwan, H.C. Tribe, N. Jacobs, N. Hancock, A.A. Qureshi, D.G. Dunlop, R.O.C. Oreffo, Regenerative medicine in lower limb reconstruction, Regen. Med. 13 (2018) 477–490. https://doi.org/10.2217/rme-2018-0011.

[10] J.J. Li, M. Ebied, J. Xu, H. Zreiqat, Current approaches to bone tissue engineering: The interface between biology and engineering, Adv. Healthc. Mater. 7 (2018) 1–8. https://doi.org/10.1002/adhm.201701061.

[11] L. Polo-Corrales, M. Latorre-Esteves, J.E. Ramirez-Vick, Scaffold design for bone regeneration, J. Nanosci. Nanotechnol. 14 (2014) 15–56. https://doi.org/10.1166/jnn.2014.9127.

[12] A. Kolk, J. Handschel, W. Drescher, D. Rothamel, F. Kloss, M. Blessmann, M. Heiland, K.D. Wolff, R. Smeets, Current trends and future perspectives of bone substitute materials - From space holders to innovative biomaterials, J. Cranio-Maxillofacial Surg. 40 (2012) 706–718. https://doi.org/10.1016/j.jcms.2012.01.002.

[13] L. Roseti, V. Parisi, M. Petretta, C. Cavallo, G. Desando, I. Bartolotti, B. Grigolo, Scaffolds for bone tissue engineering: State of the art and new perspectives, Mater. Sci. Eng. C. 78 (2017) 1246–1262. https://doi.org/10.1016/j.msec.2017.05.017.

[14] S. Wu, X. Liu, K.W.K. Yeung, C. Liu, X. Yang, Biomimetic porous scaffolds for bone tissue

engineering, Mater. Sci. Eng. R Reports. 80 (2014) 1–36. https://doi.org/10.1016/j.mser.2014.04.001.

[15] S. Arabnejad, R. Burnett Johnston, J.A. Pura, B. Singh, M. Tanzer, D. Pasini, High-strength porous biomaterials for bone replacement: A strategy to assess the interplay between cell morphology, mechanical properties, bone ingrowth and manufacturing constraints, Acta Biomater. 30 (2016) 345–356. https://doi.org/10.1016/j.actbio.2015.10.048.

[16] V. Karageorgiou, D. Kaplan, Porosity of 3D biomaterial scaffolds and osteogenesis, Biomaterials. 26 (2005) 5474–5491. https://doi.org/10.1016/j.biomaterials.2005.02.002.

[17] A.A. Zadpoor, Bone tissue regeneration: The role of scaffold geometry, Biomater. Sci. 3 (2015) 231–245. https://doi.org/10.1039/c4bm00291a.

[18] R.A. Gittens, T. Mclachlan, R. Olivares-navarrete, Y. Cai, S. Berner, R. Tannenbaum, Z. Schwartz, K.H. Sandhage, B.D. Boyan, The effects of combined micron-/submicron-scale surface roughness and nanoscale features on cell proliferation and differentiation, Biomaterials. 32 (2011) 3395–3403. https://doi.org/10.1016/j.biomaterials.2011.01.029.

[19] S. Dobbenga, L.E. Fratila-apachitei, A.A. Zadpoor, Nanopattern-induced osteogenic differentiation of stem cells – A systematic review, Acta Biomater. 46 (2016) 3–14. https://doi.org/10.1016/j.actbio.2016.09.031.

[20] A. Rodriguez-contreras, D. Guadarrama, A. Nanci, Surface nanoporosity has a greater influence on osteogenic and bacterial cell adhesion than crystallinity and wettability, Appl. Surf. Sci. 445 (2018) 255–261. https://doi.org/10.1016/j.apsusc.2018.03.150.

[21] Y.F. Zheng, X.N. Gu, F. Witte, Biodegradable metals, Mater. Sci. Eng. R. 77 (2014) 1–34. https://doi.org/10.1007/978-1-4614-3942-4_5.

[22] M.F.F.A. Hamidi, W.S.W. Harun, M. Samykano, S.A.C. Ghani, Z. Ghazalli, F. Ahmad, A.B. Sulong, A review of biocompatible metal injection moulding process parameters for biomedical applications, Mater. Sci. Eng. C. 78 (2017) 1263–1276. https://doi.org/10.1016/j.msec.2017.05.016.

[23] B. Arifvianto, J. Zhou, Fabrication of metallic biomedical scaffolds with the space holder method: A review, Materials (Basel). 7 (2014) 3588–3622. https://doi.org/10.3390/ma7053588.

[24] Y. Chen, D. Kent, M. Bermingham, A. Dehghan-Manshadi, G. Wang, C. Wen, M. Dargusch, Manufacturing of graded titanium scaffolds using a novel space holder technique, Bioact. Mater. 2 (2017) 248–252. https://doi.org/10.1016/j.bioactmat.2017.07.001.

[25] A.A. Zadpoor, J. Malda, Additive manufacturing of biomaterials, tissues, and organs, Ann. Biomed. Eng. 45 (2017) 1–11. https://doi.org/10.1007/s10439-016-1719-y.

[26] S. Bose, S. Vahabzadeh, A. Bandyopadhyay, Bone tissue engineering using 3D printing, Mater. Today. 16 (2013) 496–504. https://doi.org/10.1016/j.mattod.2013.11.017.

[27] G. Campoli, M.S. Borleffs, S. Amin Yavari, R. Wauthle, H. Weinans, A.A. Zadpoor, Mechanical properties of open-cell metallic biomaterials manufactured using additive manufacturing, Mater. Des. 49 (2013) 957–965. https://doi.org/10.1016/j.matdes.2013.01.071.

[28] S. Amin Yavari, R. Wauthle, J. Van Der Stok, A.C. Riemslag, M. Janssen, M. Mulier, J.P. Kruth, J. Schrooten, H. Weinans, A.A. Zadpoor, Fatigue behavior of porous biomaterials manufactured using selective laser melting, Mater. Sci. Eng. C. 33 (2013) 4849–4858. https://doi.org/10.1016/j.msec.2013.08.006.

[29] Y. Li, J. Zhou, P. Pavanram, M.A. Leeflang, L.I. Fockaert, B. Pouran, N. Tümer, K.U. Schröder, J.M.C. Mol, H. Weinans, H. Jahr, A.A. Zadpoor, Additively manufactured biodegradable porous magnesium, Acta Biomater. 67 (2018) 378–392. https://doi.org/10.1016/j.actbio.2017.12.008.

[30] Y. Li, H. Jahr, K. Lietaert, P. Pavanram, A. Yilmaz, L.I. Fockaert, M.A. Leeflang, B. Pouran, Y. Gonzalez-Garcia, H. Weinans, J.M.C. Mol, J. Zhou, A.A. Zadpoor, Additively manufactured biodegradable porous iron, Acta Biomater. 77 (2018) 380–393. https://doi.org/10.1016/j.actbio.2018.07.011.

[31] A. Fukuda, M. Takemoto, T. Saito, S. Fujibayashi, M. Neo, D.K. Pattanayak, T. Matsushita, K. Sasaki, N. Nishida, T. Kokubo, T. Nakamura, Osteoinduction of porous Ti implants with a channel structure fabricated by selective laser melting, Acta Biomater. 7 (2011) 2327–2336. https://doi.org/10.1016/j.actbio.2011.01.037.

[32] S. Van Bael, Y.C. Chai, S. Truscello, M. Moesen, G. Kerckhofs, H. Van Oosterwyck, J.P. Kruth, J. Schrooten, The effect of pore geometry on the in vitro biological behavior of human periosteum-derived cells seeded on selective laser-melted Ti6Al4V bone scaffolds, Acta Biomater. 8 (2012) 2824–2834. https://doi.org/10.1016/j.actbio.2012.04.001.

[33] N. Taniguchi, S. Fujibayashi, M. Takemoto, K. Sasaki, B. Otsuki, T. Nakamura, T. Matsushita, T. Kokubo, S. Matsuda, Effect of pore size on bone ingrowth into porous titanium implants fabricated by additive manufacturing: An *in vivo* experiment, Mater. Sci. Eng. C. 59 (2016) 690–701. https://doi.org/10.1016/j.msec.2015.10.069.

[34] F.A. Shah, A. Snis, A. Matic, P. Thomsen, A. Palmquist, 3D printed Ti6Al4V implant surface promotes bone maturation and retains a higher density of less aged osteocytes at the bone-implant interface, Acta Biomater. 30 (2016) 357–367. https://doi.org/10.1016/j.actbio.2015.11.013.

[35] F.A. Shah, O. Omar, F. Suska, A. Snis, A. Matic, L. Emanuelsson, B. Norlindh, J. Lausmaa, P. Thomsen, A. Palmquist, Long-term osseointegration of 3D printed CoCr constructs with an interconnected open-pore architecture prepared by electron beam melting, Acta Biomater. 36 (2016) 296–309. https://doi.org/10.1016/j.actbio.2016.03.033.

[36] D. Xiao, J. Zhang, C. Zhang, D. Barbieri, H. Yuan, L. Moroni, G. Feng, The role of calcium phosphate surface structure in osteogenesis and the mechnaism involved, Acta Biomater. (2019). https://doi.org/10.1016/j.actbio.2019.12.034.

[37] P.H. Wooley, N.J. Hallab, Wound healing, chronic inflammation, and immune responses, in: Met. Bear., Springer, New York, NY, 2014: pp. 109–133.

[38] I.A.J. van Hengel, M. Riool, L.E. Fratila-Apachitei, J. Witte-Bouma, E. Farrell, A.A. Zadpoor, S.A.J. Zaat, I. Apachitei, Selective laser melting porous metallic implants with immobilized silver nanoparticles kill and prevent biofilm formation by methicillin-resistant Staphylococcus aureus, Biomaterials. 140 (2017) 1–15. https://doi.org/10.1016/j.biomaterials.2017.02.030.

[39] A. Bandyopadhyay, B. Heer, Additive manufacturing of multi-material structures, Mater. Sci. Eng. R Reports. 129 (2018) 1–16. https://doi.org/10.1016/j.mser.2018.04.001.

[40] S. Bose, D. Ke, H. Sahasrabudhe, A. Bandyopadhyay, Additive manufacturing of biomaterials, Prog. Mater. Sci. 93 (2018) 45–111. https://doi.org/10.1016/j.pmatsci.2017.08.003.

[41] W.S.W. Harun, M.S.I.N. Kamariah, N. Muhamad, S.A.C. Ghani, F. Ahmad, Z. Mohamed, A review of

powder additive manufacturing processes for metallic biomaterials, Powder Technol. 327 (2018) 128–151. https://doi.org/10.1016/j.powtec.2017.12.058.

[42] A. Wubneh, E.K. Tsekoura, C. Ayranci, H. Uludağ, Current state of fabrication technologies and materials for bone tissue engineering, Acta Biomater. 80 (2018) 1–30. https://doi.org/10.1016/j.actbio.2018.09.031.

[43] A. Paula, M. Madrid, A. Paola, S.M. Vrech, M.A. Sanchez, Advances in additive manufacturing for bone tissue engineering scaffolds, Mater. Sci. Eng. C. 100 (2019) 631–644. https://doi.org/10.1016/j.msec.2019.03.037.

[44] L. Zhang, G. Yang, B.N. Johnson, X. Jia, Three-dimensional (3D) printed scaffold and material selection for bone repair, Acta Biomater. 84 (2019) 16–33. https://doi.org/10.1016/j.actbio.2018.11.039.

[45] X. Wang, S. Xu, S. Zhou, W. Xu, M. Leary, P. Choong, M. Qian, M. Brandt, Y. Min, Topological design and additive manufacturing of porous metals for bone scaffolds and orthopaedic implants : A review, Biomaterials. 83 (2016) 127–141. https://doi.org/10.1016/j.biomaterials.2016.01.012.

[46] X.P. Tan, Y.J. Tan, C.S.L. Chow, S.B. Tor, W.Y. Yeong, Metallic powder-bed based 3D printing of cellular scaffolds for orthopaedic implants: A state-of-the-art review on manufacturing, topological design, mechanical properties and biocompatibility, Mater. Sci. Eng. C. 76 (2017) 1328–1343. https://doi.org/10.1016/j.msec.2017.02.094.

[47] X.Y. Zhang, G. Fang, J. Zhou, Additively manufactured scaffolds for bone tissue engineering and the prediction of their mechanical behavior: A review, Materials (Basel). 10 (2017). https://doi.org/10.3390/ma10010050.

[48] A.A. Zadpoor, Additively manufactured porous metallic biomaterials, J. Mater. Chem. B. (2019). https://doi.org/10.1039/c9tb00420c.

[49] L. Yuan, S. Ding, C. Wen, Additive manufacturing technology for porous metal implant applications and triple minimal surface structures: A review, Bioact. Mater. 4 (2019) 56–70. https://doi.org/10.1016/j.bioactmat.2018.12.003.

[50] R. Singh, R. Kumar, I. Farina, F. Colangelo, L. Feo, F. Fraternali, Multi-material additive manufacturing of sustainable innovative materials and structures, Polymers (Basel). 11 (2019) 62. https://doi.org/10.3390/polym11010062.

[51] S. Dadbakhsh, R. Mertens, L. Hao, J. Van Humbeeck, J.P. Kruth, Selective laser melting to manufacture "in situ" metal matrix composites: A review, Adv. Eng. Mater. 21 (2019) 1–18. https://doi.org/10.1002/adem.201801244.

[52] E. Fereiduni, M. Yakout, M. Elbestawi, Laser-based additive manufacturing of lightweight metal matrix composites, in: B. Almangour (Ed.), Addit. Manuf. Emerg. Mater., Springer, Cham, 2019: pp. 55–109.

[53] T. Larimian, T. Borkar, Additive manufacturing of in situ metal matrix composites, in: B. Almangour (Ed.), Addit. Manuf. Emerg. Mater., Springer, Cham, 2019: pp. 1–28.

[54] ASTM F2792-12, Standard Terminology for Additive Manufacturing Technologies, ASTM Int. (2012).

[55] D. Gu, Y.C. Hagedorn, W. Meiners, K. Wissenbach, R. Poprawe, Selective laser melting of in-situ TiC/Ti5Si3 composites with novel reinforcement architecture and elevated performance, Surf. Coatings Technol. 205 (2011) 3285–3292. https://doi.org/10.1016/j.surfcoat.2010.11.051.

[56] D. Gu, C. Hong, G. Meng, Densification, microstructure, and wear property of in situ titanium nitride-

reinforced titanium silicide matrix composites prepared by a novel selective laser melting process, Metall. Mater. Trans. A Phys. Metall. Mater. Sci. 43 (2012) 697–708. https://doi.org/10.1007/s11661-011-0876-8.

[57] C. Cai, C. Radoslaw, J. Zhang, Q. Yan, S. Wen, B. Song, Y. Shi, In-situ preparation and formation of TiB/Ti-6Al-4V nanocomposite via laser additive manufacturing: Microstructure evolution and tribological behavior, Powder Technol. 342 (2019) 73–84. https://doi.org/10.1016/j.powtec.2018.09.088.

[58] H. Attar, M. Bönisch, M. Calin, L.C. Zhang, S. Scudino, J. Eckert, Selective laser melting of in situ titanium-titanium boride composites: Processing, microstructure and mechanical properties, Acta Mater. 76 (2014) 13–22. https://doi.org/10.1016/j.actamat.2014.05.022.

[59] C. Han, Q. Wang, B. Song, W. Li, Q. Wei, S. Wen, J. Liu, Y. Shi, Microstructure and property evolutions of titanium/nano-hydroxyapatite composites in-situ prepared by selective laser melting, J. Mech. Behav. Biomed. Mater. 71 (2017) 85–94. https://doi.org/10.1016/j.jmbbm.2017.02.021.

[60] C. Han, Y. Li, Q. Wang, D. Cai, Q. Wei, L. Yang, S. Wen, Titanium/hydroxyapatite (Ti/HA) gradient materials with quasi-continuous ratios fabricated by SLM: Material interface and fracture toughness, Mater. Des. 141 (2018) 256–266. https://doi.org/10.1016/j.matdes.2017.12.037.

[61] B. Vrancken, L. Thijs, J.P. Kruth, J. Van Humbeeck, Microstructure and mechanical properties of a novel β titanium metallic composite by selective laser melting, Acta Mater. 68 (2014) 150–158. https://doi.org/10.1016/j.actamat.2014.01.018.

[62] J.C. Wang, Y.J. Liu, P. Qin, S.X. Liang, T.B. Sercombe, L.C. Zhang, Selective laser melting of Ti–35Nb composite from elemental powder mixture: Microstructure, mechanical behavior and corrosion behavior, Mater. Sci. Eng. A. 760 (2019) 214–224. https://doi.org/10.1016/j.msea.2019.06.001.

[63] M. Fischer, D. Joguet, G. Robin, L. Peltier, P. Laheurte, In situ elaboration of a binary Ti-26Nb alloy by selective laser melting of elemental titanium and niobium mixed powders, Mater. Sci. Eng. C. 62 (2016) 852–859. https://doi.org/10.1016/j.msec.2016.02.033.

[64] S.L. Sing, W.Y. Yeong, F.E. Wiria, Selective laser melting of titanium alloy with 50 wt% tantalum: Microstructure and mechanical properties, J. Alloys Compd. 660 (2016) 461–470. https://doi.org/10.1016/j.jallcom.2015.11.141.

[65] S. Guo, Y. Lu, S. Wu, L. Liu, M. He, C. Zhao, Y. Gan, J. Lin, J. Luo, X. Xu, J. Lin, Preliminary study on the corrosion resistance , antibacterial activity and cytotoxicity of selective-laser-melted Ti6Al4V-xCu alloys, Mater. Sci. Eng. C. 72 (2017) 631–640. https://doi.org/10.1016/j.msec.2016.11.126.

[66] X. Xu, Y. Lu, S. Li, S. Guo, M. He, K. Luo, J. Lin, Copper-modified Ti6Al4V alloy fabricated by selective laser melting with pro-angiogenic and anti-inflammatory properties for potential guided bone regeneration applications, Mater. Sci. Eng. C. 90 (2018) 198–210. https://doi.org/10.1016/j.msec.2018.04.046.

[67] K. Wei, X. Zeng, Z. Wang, J. Deng, M. Liu, G. Huang, X. Yuan, Selective laser melting of Mg-Zn binary alloys: Effects of Zn content on densification behavior, microstructure, and mechanical property, Mater. Sci. Eng. A. 756 (2019) 226–236. https://doi.org/10.1016/j.msea.2019.04.067.

[68] C. Shuai, Y. Yang, S. Peng, C. Gao, P. Feng, J. Chen, Y. Liu, X. Lin, S. Yang, F. Yuan, Nd-induced honeycomb structure of intermetallic phase enhances the corrosion resistance of Mg alloys for bone

implants, J. Mater. Sci. Mater. Med. 28 (2017). https://doi.org/10.1007/s10856-017-5945-0.

[69] T. Long, X. Zhang, Q. Huang, L. Liu, Y. Liu, J. Ren, Y. Yin, D. Wu, H. Wu, Novel Mg-based alloys by selective laser melting for biomedical applications: microstructure evolution, microhardness and in vitro degradation behaviour, Virtual Phys. Prototyp. 13 (2018) 71–81. https://doi.org/10.1080/17452759.2017.1411662.

[70] C. Shuai, L. Liu, M. Zhao, P. Feng, Y. Yang, W. Guo, C. Gao, F. Yuan, Microstructure, biodegradation, antibacterial and mechanical properties of ZK60-Cu alloys prepared by selective laser melting technique, J. Mater. Sci. Technol. 34 (2018) 1944–1952. https://doi.org/10.1016/j.jmst.2018.02.006.

[71] D. Carluccio, C. Xu, J. Venezuela, Y. Cao, D. Kent, M. Bermingham, A.G. Demir, B. Previtali, Q. Ye, M. Dargusch, Additively manufactured iron-manganese for biodegradable porous load-bearing bone scaffold applications, (2019) 1–15. https://doi.org/10.1016/j.actbio.2019.12.018.

[72] C. Shuai, W. Yang, Y. Yang, H. Pan, C. He, F. Qi, D. Xie, H. Liang, Selective laser melted Fe-Mn bone scaffold: microstructure, corrosion behavior and cell response, Mater. Res. Express. 7 (2019).

[73] Y. Hu, B. Zhao, F. Ning, H. Wang, W. Cong, In-situ ultrafine three-dimensional quasi-continuous network microstructural TiB reinforced titanium matrix composites fabrication using laser engineered net shaping, Mater. Lett. 195 (2017) 116–119. https://doi.org/10.1016/j.matlet.2017.02.112.

[74] Y. Hu, F. Ning, H. Wang, W. Cong, B. Zhao, Laser engineered net shaping of quasi-continuous network microstructural TiB reinforced titanium matrix bulk composites: Microstructure and wear performance, Opt. Laser Technol. 99 (2018) 174–183. https://doi.org/10.1016/j.optlastec.2017.08.032.

[75] H. Sahasrabudhe, A. Bandyopadhyay, In situ reactive multi-material Ti6Al4V-calcium phosphate-nitride coatings for bio-tribological applications, J. Mech. Behav. Biomed. Mater. 85 (2018) 1–11. https://doi.org/10.1016/j.jmbbm.2018.05.020.

[76] A. Bandyopadhyay, S. Dittrick, T. Gualtieri, J. Wu, W.M.K. Biomedical, M. Engineering, Calcium phosphate–titanium composites for articulating surfaces of load-bearing implants, J. Mech. Behav. Biomed. Mater. 57 (2016) 280–288. https://doi.org/10.1016/j.jmbbm.2015.11.022.

[77] S. Samuel, S. Nag, S. Nasrazadani, V. Ukirde, M. El Bouanani, A. Mohandas, K. Nguyen, R. Banerjee, Corrosion resistance and in vitro response of laser-deposited Ti-Nb-Zr-Ta alloys for orthopedic implant applications, J. Biomed. Mater. Res. - Part A. 94 (2010) 1251–1256. https://doi.org/10.1002/jbm.a.32782.

[78] K.D. Traxel, A. Bandyopadhyay, Reactive-deposition-based additive manufacturing of Ti-Zr-BN composites, Addit. Manuf. 24 (2018) 353–363. https://doi.org/10.1016/j.addma.2018.10.005.

[79] B. Vamsi Krishna, W. Xue, S. Bose, A. Bandyopadhyay, Functionally graded Co-Cr-Mo coating on Ti-6Al-4V alloy structures, Acta Biomater. 4 (2008) 697–706. https://doi.org/10.1016/j.actbio.2007.10.005.

[80] V.K. Balla, P.D. DeVasConCellos, W. Xue, S. Bose, A. Bandyopadhyay, Fabrication of compositionally and structurally graded Ti-TiO2 structures using laser engineered net shaping (LENS), Acta Biomater. 5 (2009) 1831–1837. https://doi.org/10.1016/j.actbio.2009.01.011.

[81] F.H. Froes, B. Dutta, The additive manufacturing (AM) of titanium alloys, Adv. Mater. Res. 1019 (2014) 19–25. https://doi.org/10.1016/B978-0-12-800054-0.00024-1.

[82] G.D.J. Ram, C. Robinson, Y. Yang, B.E. Stucker, Use of ultrasonic consolidation for fabrication of multi-material structures, Rapid Prototyp. J. 13 (2007) 226–235.

https://doi.org/10.1108/13552540710776179.

[83] J.O. Obielodan, A. Ceylan, L.E. Murr, B.E. Stucker, Multi-material bonding in ultrasonic consolidation, Rapid Prototyp. J. 16 (2010) 180–188. https://doi.org/10.1108/13552541011034843.

[84] J. Obielodan, B. Stucker, A fabrication methodology for dual-material engineering structures using ultrasonic additive manufacturing, Int. J. Adv. Manuf. Technol. (2014) 277–284. https://doi.org/10.1007/s00170-013-5266-5.

[85] Y. Bai, C.B. Williams, Binder jetting additive manufacturing with a particle-free metal ink as a binder precursor, Mater. Des. 147 (2018) 146–156. https://doi.org/10.1016/j.matdes.2018.03.027.

[86] D.T. Chou, D. Wells, D. Hong, B. Lee, H. Kuhn, P.N. Kumta, Novel processing of iron-manganese alloy-based biomaterials by inkjet 3-D printing, Acta Biomater. 9 (2013) 8593–8603. https://doi.org/10.1016/j.actbio.2013.04.016.

[87] D. Hong, D.T. Chou, O.I. Velikokhatnyi, A. Roy, B. Lee, I. Swink, I. Issaev, H.A. Kuhn, P.N. Kumta, Binder-jetting 3D printing and alloy development of new biodegradable Fe-Mn-Ca/Mg alloys, Acta Biomater. 45 (2016) 375–386. https://doi.org/10.1016/j.actbio.2016.08.032.

[88] J.A. Lewis, Direct ink writing of 3D functional materials, Adv. Funct. Mater. 16 (2006) 2193–2204. https://doi.org/10.1002/adfm.200600434.

[89] H. Ma, T. Li, Z. Huan, M. Zhang, Z. Yang, J. Wang, J. Chang, C. Wu, 3D printing of high-strength bioscaffolds for the synergistic treatment of bone cancer, NPG Asia Mater. 10 (2018) 31–44. https://doi.org/10.1038/s41427-018-0015-8.

[90] A.E. Jakus, S.L. Taylor, N.R. Geisendorfer, D.C. Dunand, R.N. Shah, Metallic Architectures from 3D-Printed Powder-Based Liquid Inks, Adv. Funct. Mater. 25 (2015) 6985–6995. https://doi.org/10.1002/adfm.201503921.

[91] A.E. Jakus, A.L. Rutz, S.W. Jordan, A. Kannan, S.M. Mitchell, C. Yun, K.D. Koube, S.C. Yoo, H.E. Whiteley, C.P. Richter, R.D. Galiano, W.K. Hsu, S.R. Stock, E.L. Hsu, R.N. Shah, Hyperelastic "bone": A highly versatile, growth factor-free, osteoregenerative, scalable, and surgically friendly biomaterial, Sci. Transl. Med. 8 (2016) 1–16. https://doi.org/10.1126/scitranslmed.aaf7704.

[92] B.S.L. Taylor, A.E. Jakus, R.N. Shah, D.C. Dunand, Iron and nickel cellular structures by sintering of 3D-printed oxide or metallic particle inks, Adv. Eng. Mater. (2016) 1–8. https://doi.org/10.1002/adem.201600365.

[93] A.E. Jakus, K.D. Koube, N.R. Geisendorfer, R.N. Shah, Robust and elastic lunar and martian structures from 3D-printed regolith inks, Sci. Rep. 7 (2017) 44931. https://doi.org/10.1038/srep44931.

[94] A.E. Jakus, E.B. Secor, A.L. Rutz, S.W. Jordan, M.C. Hersam, R.N. Shah, Three-dimensional printing of high-content graphene scaffolds for electronic and biomedical applications, ACS Nano. 9 (2015) 4636–4648. https://doi.org/10.1021/acsnano.5b01179.

[95] F. Li, J. Li, H. Kou, G. Xu, T. Li, L. Zhou, Anisotropic porous titanium with superior mechanical compatibility in the range of physiological strain rate for trabecular bone implant applications, Mater. Lett. 137 (2014) 424–427. https://doi.org/10.1016/j.matlet.2014.09.047.

[96] R. Wauthle, S.M. Ahmadi, S. Amin Yavari, M. Mulier, A.A. Zadpoor, H. Weinans, J. Van Humbeeck, J.P. Kruth, J. Schrooten, Revival of pure titanium for dynamically loaded porous implants using additive manufacturing, Mater. Sci. Eng. C. 54 (2015) 94–100. https://doi.org/10.1016/j.msec.2015.05.001.

[97] W. Xu, M. Brandt, S. Sun, J. Elambasseril, Q. Liu, K. Latham, K. Xia, M. Qian, Additive manufacturing of strong and ductile Ti-6Al-4V by selective laser melting via in situ martensite decomposition, Acta Mater. 85 (2015) 74–84. https://doi.org/10.1016/j.actamat.2014.11.028.

[98] F. Li, J. Li, H. Kou, L. Zhou, Porous Ti6Al4V alloys with enhanced normalized fatigue strength for biomedical applications, Mater. Sci. Eng. C. 60 (2016) 485–488. https://doi.org/10.1016/j.msec.2015.11.074.

[99] F. Li, J. Li, T. Huang, H. Kou, L. Zhou, Compression fatigue behavior and failure mechanism of porous titanium for biomedical applications, J. Mech. Behav. Biomed. Mater. 65 (2017) 814–823. https://doi.org/10.1016/j.jmbbm.2016.09.035.

[100] F.S.L. Bobbert, A.A. Zadpoor, Effects of bone substitute architecture and surface properties on cell response, angiogenesis, and structure of new bone, J. Mater. Chem. B. (2017). https://doi.org/10.1039/c7tb00741h.

[101] X.-Y. Zhang, G. Fang, S. Leeflang, A.A. Zadpoor, J. Zhou, Topological design, permeability and mechanical behavior of additively manufactured functionally graded porous metallic biomaterials, Acta Biomater. 84 (2018) 437–452. https://doi.org/10.1016/j.actbio.2018.12.013.

[102] A.A. Zadpoor, Design for additive bio-manufacturing: From patient-specific medical devices to rationally designed meta-biomaterials, Int. J. Mol. Sci. (2017). https://doi.org/10.3390/ijms18081607.

[103] H.R. Cho, T.S. Roh, K.W. Shim, Y.O. Kim, D.H. Lew, I.S. Yun, Skull reconstruction with custom made three-dimensional titanium implant, Arch. Craniofacial Surg. 16 (2015) 11. https://doi.org/10.7181/acfs.2015.16.1.11.

[104] E.K. Park, J.Y. Lim, I.S. Yun, J.S. Kim, S.H. Woo, D.S. Kim, K.W. Shim, Cranioplasty enhanced by three-dimensional printing: Custom-made three-dimensional-printed titanium implants for skull defects, J. Craniofac. Surg. 27 (2016) 943–949. https://doi.org/10.1097/SCS.0000000000002656.

[105] K.S. Hamid, S.G. Parekh, S.B. Adams, Salvage of Severe Foot and Ankle Trauma with a 3D Printed Scaffold, Foot Ankle Int. 37 (2016) 433–439. https://doi.org/10.1177/1071100715620895.

[106] T.J. Dekker, J.R. Steele, A.E. Federer, K.S. Hamid, S.B. Adams, Use of patient-specific 3D-printed titanium implants for complex foot and ankle limb salvage, deformity correction, and arthrodesis procedures, Foot Ankle Int. 39 (2018) 916–921. https://doi.org/10.1177/1071100718770133.

[107] T.X. Han, B. Chang, X. Ding, G.N. Yue, W. Song, H.P. Tang, L. Jia, L.Z. Zhao, Y.M. Zhang, Improved bone formation and ingrowth for additively manufactured porous Ti6Al4V bone implants with strontium laden nanotube array coating, RSC Adv. 6 (2016) 13686–13697. https://doi.org/10.1039/c5ra20370h.

[108] D. Zhao, F. Witte, F. Lu, J. Wang, J. Li, L. Qin, Current status on clinical applications of magnesium-based orthopaedic implants : A review from clinical translational perspective, Biomaterials. 112 (2017) 287–302. https://doi.org/10.1016/j.biomaterials.2016.10.017.

[109] P. Wan, L. Tan, K. Yang, Surface modification on biodegradable magnesium alloys as orthopedic implant materials to improve the bio-adaptability: A review, J. Mater. Sci. Technol. 32 (2016) 827–834. https://doi.org/10.1016/j.jmst.2016.05.003.

[110] D. Noviana, D. Paramitha, M. Fakhrul, H. Hermawan, The effect of hydrogen gas evolution of magnesium implant on the postimplantation mortality of rats, J. Orthop. Transl. 5 (2016) 9–15.

https://doi.org/10.1016/j.jot.2015.08.003.

[111] Q. Wang, L. Tan, W. Xu, B. Zhang, K. Yang, Dynamic behaviors of a Ca-P coated AZ31B magnesium alloy during in vitro and *in vivo* degradations, Mater. Sci. Eng. B. 176 (2011) 1718–1726. https://doi.org/10.1016/j.mseb.2011.06.005.

[112] J. Gan, L. Tan, K. Yang, Z. Hu, Bioactive Ca–P coating with self-sealing structure on pure magnesium, J. Mater. Sci. Mater. Med. 24 (2013) 889–901. https://doi.org/10.1007/s10856-013-4850-4.

[113] L. Tan, Q. Wang, X. Lin, P. Wan, G. Zhang, Q. Zhang, K. Yang, Loss of mechanical properties *in vivo* and bone – implant interface strength of AZ31B magnesium alloy screws with Si-containing coating, Acta Biomater. 10 (2014) 2333–2340. https://doi.org/10.1016/j.actbio.2013.12.020.

[114] L. Yang, N. Hort, D. Laipple, D. Höche, Y. Huang, K.U. Kainer, R. Willumeit, F. Feyerabend, Element distribution in the corrosion layer and cytotoxicity of alloy Mg-10Dy during in vitro biodegradation, Acta Biomater. 9 (2013) 8475–8487. https://doi.org/10.1016/j.actbio.2012.10.001.

[115] H. Miao, D. Zhang, C. Chen, L. Zhang, J. Pei, Y. Su, H. Huang, Z. Wang, B. Kang, W. Ding, H. Zeng, G. Yuan, Research on biodegradable Mg-Zn-Gd alloys for potential orthopedic implants: *In vitro* and *in viv*o evaluations, ACS Biomater. Sci. Eng. 5 (2019) 1623–1634. https://doi.org/10.1021/acsbiomaterials.8b01563.

[116] J. Niu, M. Xiong, X. Guan, J. Zhang, H. Huang, J. Pei, The *in vivo* degradation and bone-implant interface of Mg-Nd-Zn-Zr alloy screws : 18 months post-operation results, Corros. Sci. 113 (2016) 183–187. https://doi.org/10.1016/j.corsci.2016.10.009.

[117] D. Chou, D. Hong, S. Oksuz, R. Schweizer, A. Roy, B. Lee, P. Shridhar, V. Gorantla, Corrosion and bone healing of Mg-Y-Zn-Zr-Ca alloy implants: Comparative *in vivo* study in a non-immobilized rat femoral fracture model, J. Biomater. Appl. (2019) 1–17. https://doi.org/10.1177/0885328219825568.

[118] T. Kraus, S.F. Fischerauer, A.C. Hänzi, P.J. Uggowitzer, J.F. Löffler, A.M. Weinberg, Magnesium alloys for temporary implants in osteosynthesis: *In vivo* studies of their degradation and interaction with bone, Acta Biomater. 8 (2012) 1230–1238. https://doi.org/10.1016/j.actbio.2011.11.008.

[119] H. Windhagen, K. Radtke, A. Weizbauer, J. Diekmann, Y. Noll, U. Kreimeyer, R. Schavan, C. Stukenborg-colsman, H. Waizy, Biodegradable magnesium-based screw clinically equivalent to titanium screw in hallux valgus surgery : short term results of the first prospective , randomized , controlled clinical pilot study, Biomed. Eng. Online. 12 (2013) 1–10.

[120] J. Lee, H. Han, K. Han, J. Park, H. Jeon, M. Ok, Long-term clinical study and multiscale analysis of *in vivo* biodegradation mechanism of Mg alloy, Proc. Natl. Acad. Sci. 113 (2016) 716–721. https://doi.org/10.1073/pnas.1518238113.

[121] D. Zhao, S. Huang, F. Lu, B. Wang, L. Yang, L. Qin, K. Yang, Y. Li, W. Li, W. Wang, S. Tian, X. Zhang, W. Gao, Z. Wang, Y. Zhang, X. Xie, J. Wang, J. Li, Vascularized bone grafting fixed by biodegradable magnesium screw for treating osteonecrosis of the femoral head, Biomaterials. 81 (2016) 84–92. https://doi.org/10.1016/j.biomaterials.2015.11.038.

[122] M. Salehi, S. Maleksaeedi, S.M.L. Nai, G.K. Meenashisundaram, M.H. Goh, M. Gupta, A paradigm shift towards compositionally zero-sum binderless 3D printing of magnesium alloys via capillary-mediated bridging, Acta Mater. 165 (2019) 294–306. https://doi.org/10.1016/j.actamat.2018.11.061.

[123] M. Salehi, S. Maleksaeedi, M.A. Bin Sapari, S.M.L. Nai, G.K. Meenashisundaram, M. Gupta, Additive

manufacturing of magnesium-zinc-zirconium (ZK) alloys via capillary-mediated binderless three-dimensional printing, Mater. Des. 169 (2019) 107683. https://doi.org/10.1016/j.matdes.2019.107683.

[124] R. Gorejová, L. Haverová, R. Oriňaková, A. Oriňak, M. Oriňak, Recent advancements in Fe-based biodegradable materials for bone repair, J. Mater. Sci. 54 (2019) 1913–1947. https://doi.org/10.1007/s10853-018-3011-z.

[125] J. He, F.L. He, D.W. Li, Y.L. Liu, Y.Y. Liu, Y.J. Ye, D.C. Yin, Advances in Fe-based biodegradable metallic materials, RSC Adv. 6 (2016) 112819–112838. https://doi.org/10.1039/C6RA20594A.

[126] Q. Zhang, P. Cao, Degradable porous Fe-35wt.% Mn produced via powder sintering from NH4NHCO3 porogen, Mater. Chem. Phys. 163 (2015) 394–401. https://doi.org/10.1016/j.matchemphys.2015.07.056.

[127] M. Kupková, M. Hrubovčáková, M. Kupka, R. Oriňáková, Sintering behaviour, graded microstructure and corrosion performance of sintered Fe-Mn biomaterials, Int. J. Electrochem. Sci. 10 (2015) 9256–9268.

[128] M. Heiden, E. Walker, E. Nauman, L. Stanciu, Evolution of novel bioresorbable iron-manganese implant surfaces and their degradation behaviors in vitro, J. Biomed. Mater. Res. Part A. 103 (2015) 185–193. https://doi.org/10.1002/jbm.a.35155.

[129] H. Hermawan, H. Alamdari, D. Mantovani, D. Dube, Iron-manganese : new class of metallic degradable biomaterials prepared by powder metallurgy, Powder Metall. 51 (2008). https://doi.org/10.1179/174329008X284868.

[130] J.H. Beattie, A. Avenell, Trace element nutrition and bone metabolism, Nutr. Res. Rev. 5 (1992) 167–188.

[131] J. Čapek, K. Stehlíková, A. Michalcová, Š. Msallamová, D. Vojtěch, Microstructure, mechanical and corrosion properties of biodegradable powder metallurgical Fe-2 wt% X (X = Pd, Ag and C) alloys, Mater. Chem. Phys. 181 (2016) 501–511. https://doi.org/10.1016/j.matchemphys.2016.06.087.

[132] T. Huang, J. Cheng, D. Bian, Y. Zheng, Fe-Au and Fe-Ag composites as candidates for biodegradable stent materials, J. Biomed. Mater. Res. - Part B Appl. Biomater. 104 (2015) 225–240. https://doi.org/10.1002/jbm.b.33389.

[133] T. Huang, J. Cheng, Y.F. Zheng, In vitro degradation and biocompatibility of Fe-Pd and Fe-Pt composites fabricated by spark plasma sintering, Mater. Sci. Eng. C. 35 (2014) 43–53. https://doi.org/10.1016/j.msec.2013.10.023.

[134] M.F. Ulum, A.K. Nasution, A.H. Yusop, A. Arafat, M.R.A. Kadir, V. Juniantito, D. Noviana, H. Hermawan, Evidences of *in vivo* bioactivity of Fe-bioceramic composites for temporary bone implants, J. Biomed. Mater. Res. - Part B Appl. Biomater. (2014). https://doi.org/10.1002/jbm.b.33315.

[135] D. Noviana, S. Estuningsih, D. Paramitha, M. Fakhrul Ulum, H. Hermawan, In-vitro cytotoxicity and in-vivo tissue response study of foreign bodies iron based materials, Adv. Mater. Res. 1112 (2015) 449–452. https://doi.org/10.4028/www.scientific.net/amr.1112.449.

[136] T. Kraus, F. Moszner, S. Fischerauer, M. Fiedler, E. Martinelli, J. Eichler, F. Witte, E. Willbold, M. Schinhammer, M. Meischel, P.J. Uggowitzer, J.F. Löffler, A. Weinberg, Biodegradable Fe-based alloys for use in osteosynthesis: Outcome of an in vivo study after 52 weeks, Acta Biomater. 10 (2014) 3346–3353. https://doi.org/10.1016/j.actbio.2014.04.007.

[137] M. Traverson, M. Heiden, L.A. Stanciu, E.A. Nauman, Y. Jones-hall, G.J. Breur, In vivo evaluation of

biodegradability and biocompatibility of Fe30Mn alloy, Vet. Comp. Orthop. Traumatol. 31 (2018) 10–16.

[138] M. Fântânariu, L.C. Trinc, C. Solcan, A. Trofin, E.V. S, S. Stanciu, A new Fe-Mn-Si alloplastic biomaterial as bone grafting material: *In vivo* study, Appl. Surf. Sci. 352 (2015) 129–139. https://doi.org/10.1016/j.apsusc.2015.04.197.

[139] Y.P. Feng, A. Blanquer, J. Fornell, H. Zhang, P. Solsona, M.D. Baró, S. Suriñach, E. Ibáñez, E. García-Lecina, X. Wei, R. Li, L. Barrios, E. Pellicer, C. Nogues, J. Sort, Novel Fe-Mn-Si-Pd alloys: Insights into mechanical, magnetic, corrosion resistance and biocompatibility performances, R. Soc. Chem. 4 (2016) 6402–6412. https://doi.org/10.1039/c6tb01951j.

[140] H. Do Cha, J.M. Hong, T.Y. Kang, J.W. Jung, D.H. Ha, D.W. Cho, Effects of micro-patterns in three-dimensional scaffolds for tissue engineering applications, J. Micromechanics Microengineering. (2012). https://doi.org/10.1088/0960-1317/22/12/125002.

[141] T. Sjöström, L.E. Mcnamara, R.M.D. Meek, M.J. Dalby, B. Su, 2D and 3D nanopatterning of titanium for enhancing osteoinduction of stem cells at implant surfaces, Adv. Healthc. Mater. (2013). https://doi.org/10.1002/adhm.201200353.

[142] D.S. Widyaratih, P.L. Hagedoorn, L.G. Otten, M. Ganjian, N. Tümer, I. Apachitei, C.W. Hagen, L.E. Fratila-Apachitei, A.A. Zadpoor, Towards osteogenic and bactericidal nanopatterns?, Nanotechnology. (2019). https://doi.org/10.1088/1361-6528/ab0a3a.

FIGURE CAPTIONS

Figure 1. The anatomy of bone (Reproduced with permission from [1]).

Figure 2. Laser and ultrasonic multi-material AM for metals according to the process classifications of ASTM F2792−12a [54]: (a) powder bed fusion, (b) directed energy deposition, and (c) sheet lamination.

Figure 3. Adhesive multi-material AM for metals according to the process classifications of ASTM F2792−12a [54]: (a) binder jetting and (b) material extrusion.

Figure 4. AM of Ti-based biomaterials. (a) Porous AM Ti-6Al-4V biomaterials with triply periodic minimal surfaces (1.5 mm unit cells; cylindrical specimens with a height of 20 mm and a diameter of 15 mm). (Reprinted from [100] with permission from the Royal Society of Chemistry). (b) A patient-specific implant fabricated using SLM based on computed-tomography (CT) images (Reprinted with permission from [102]). (c) Surface-biofunctionalized AM porous Ti-6Al-4V integrates (i) Ag nanoparticles on the surface and (ii) significantly reduces the number of MRSA *ex vivo*, while (iii) increasing the viability of human MSCs *in vitro*, as compared with the non-treated surface (calcein acetoxymethyl and ethidium homodimer-1 stain). (Reprinted from [38] with permission from Elsevier).

Figure 5. Microstructure of multi-functional AM Ti-based biomaterials. (a) The dendrite-shaped TiC grains on TiC-Ti_5Si_3 composites vary in size, when fabricated with different laser scanning parameters (Reprinted from [55] with permission from Elsevier). (b) A uniform distribution of eutectic TiB grains on Ti-TiB composites is obtained at a higher laser power (Reprinted from [73] with permission from Elsevier). (c) The grain refinement of Ti-HA composites occurs as the HA content increases (Reprinted from [59] with permission from Elsevier). (d) *In situ* AM of Ti and Ta transforms the α phase Ti into the β phase,

lowering the Young's modulus of Ti, while modifying its grain morphology (Reprinted from [64] with permission from Elsevier).

Figure 6. Biological performance of *in situ* AM Ti-6Al-4V-6Cu in terms of osteogenic response, inflammatory response, angiogenesis, and antibacterial properties (Reprinted from [65,66] with permission from Elsevier). (a) The viability of osteoblasts and (b) ALP activity on Ti-6Al-4V-6Cu are comparable to those of Ti-6Al-4V. (c) Macrophages are less active on Ti-6Al-4V-6Cu and (d) demonstrate a lower degree of expression of pro-inflammatory IL-6 markers. (e) HUVECs show a well-spread morphology on Ti-6Al-4V-Cu and (f) upregulate the expression of angiogenesis-related VEGF-A [66]. (g) Ti-6Al-4V-6Cu significantly reduces the number of *E. coli* and *S. aureus in vitro* culture in Petri dish (h) with an antibacterial rate of 99.99% [65]. The osteoblasts, macrophages, and HUVECs were stained using phalloidin (red) and 4',6-diamidino-2-phenylindole (blue).

Figure 7. Mg-based biomaterials: *In vivo* test and clinical study. (a) Histological images with Levai-Laczko staining show the distinct *in vivo* biodegradation profiles of ZX50 and WZ21 (two Mg alloy specimens with a cylindrical shape, a diameter of 1.6 mm and a length of 8 mm) for up to 36 weeks (Reprinted from [118] with permission from Elsevier). WZ21 presents a combination of an appropriate degradation rate, mechanical integrity, and enhanced bone tissue regeneration performance. (b) Complete biodegradation of Mg-Ca-Zn screws (with a diameter of 2.3 mm and a length of 14 mm) and the regeneration of distal radius fracture after 12 months of implantation (Reproduced from [120]).

Figure 8. AM of Mg-based biomaterials. SLM WE43 with a topologically-ordered open porosity (cylindrical scaffold specimens with a diameter of 10 mm and a height of 11.2 mm) shows (a) negligible structural disintegration after 4 weeks of *in vitro* biodegradation and (b) maintains its Young's modulus and (c) yield strength in the range of the mechanical properties of trabecular bone (Reprinted from [29] with permission from Elsevier). A

capillary-mediated binderless AM ZK alloy in (d) the green condition, with (e) a SEM micrograph of the bonding bridge between ZK particles. (f) The subsequent post-AM heat-treatment enables fine-tuning of the mechanical properties of the AM ZK alloy based on the adjustment of sintering parameters (Reprinted from [123] with permission from Elsevier).

Figure 9. Multi-functional AM Mg-based biomaterials. (a) The mechanical properties of *in situ* SLM of binary Mg-Zn alloys, where a high relative density is only achieved through the *in situ* alloying of Mg-1Zn (the scale bars labeled with a length of 500 μm) (Reprinted from [67] with permission from Elsevier). (b) A schematic illustration of a controlled biodegradation profile due to the formation of Mg-Zn-Nd intermetallic phases along the α-Mg grain boundaries. (c) *In situ* SLM ZK60-0.4Cu alloys maintain a low weight loss rate during biodegradation, while demonstrating (d) antibacterial properties against *E. coli* (Reprinted from [70] with permission from Elsevier).

Figure 10. Fe-based biomaterials: *In vivo* biodegradation and biocompatibility. (a) Neither structural changes (b) nor significant weight losses of cylindrical Fe-based biomaterials (specimens with a diameter of 1.6 mm and a length of 8 mm) were observed after a 52-week *in vivo* test (Reprinted from [136] with permission from Elsevier). (c) Detection of Fe^{2+}/Fe^{3+} (Quincke stain), Fe^{2+} (Turnbull Blue stain) and Fe^{3+} (Prussian Blue stain) in the vicinity of pure Fe (*vicinity in vivo*) (Reprinted from [136] with permission from Elsevier). (d) A histological analysis (in hematoxylin and eosin staining) of (i, ii) pure Fe, (iii, iv) Fe-HA, (v, vi) Fe-TCP, and (vii, viii) Fe-BCP, after a 70-day *in vivo* test. ∆ – bone, ☆ – void after implant removal, ⇧ – macrophages, ◇ – granular tissue and ○ – fibrous tissue (Reprinted from [134] © 2014 Wiley Periodicals, Inc.). (e) Bone remodeling occurs during the *in vivo* tests of Fe-Mn-Si alloys (periodic acid–Schiff stain). After two weeks, (i) a small bone necrosis region (black arrow, ×100) and (ii) empty lacunae (black arrow) with some osteocytes (white arrow) were found in bigger trabeculae (×900). After 4 weeks, (iii) new

osteoid tissue and osteoblasts (black arrow) were present in the trabecular bone (×900) (Reprinted from [138] with permission from Elsevier).

Figure 11. AM of Fe-based biomaterials. (a) The porous morphologies of *ex situ* binder-jetted Fe-Mn and Fe-Mn-1Ca alloys, (b) the Fe-Mn-1Ca alloy having a higher electrochemical corrosion rate than the Fe-Mn alloy (Reprinted from [87] with permission from Elsevier). (c) Open porous topologically-ordered AM pure Fe improves (d) the electrochemical corrosion rate and (e) reduces the impedance values as compared to cold-rolled Fe. (f) The visual changes of AM pure Fe (cylindrical scaffold sample with a diameter of 10 mm and a height of 10.5 mm) during 4 weeks of *in vitro* immersion tests, where corrosion products become denser over time and envelop the open porous structure of the biomaterial (Reprinted from [30] with permission from Elsevier).

Figure 12. Multi-functional AM Fe-based biomaterials. The phase transformation of (a) α-Fe and α-Mn into the anti-ferromagnetic ε-martensite and γ-austenite Fe-Mn phases after sintering (Reprinted from [86] with permission from Elsevier). (b) *Ex situ* binder-jetted Fe-Mn and Fe-Mn-Ca alloys exhibit an anti-ferromagnetic γ-austenite Fe-Mn phase (Reprinted from [87] with permission from Elsevier). Fe-$CaSiO_3$ composites (c) stimulate the osteogenic response of the biomaterials *in vivo*, as compared to pure Fe and (d) are capable of reducing the growth of bone tumors when combined with laser treatments and ROS [89].

Figure 1

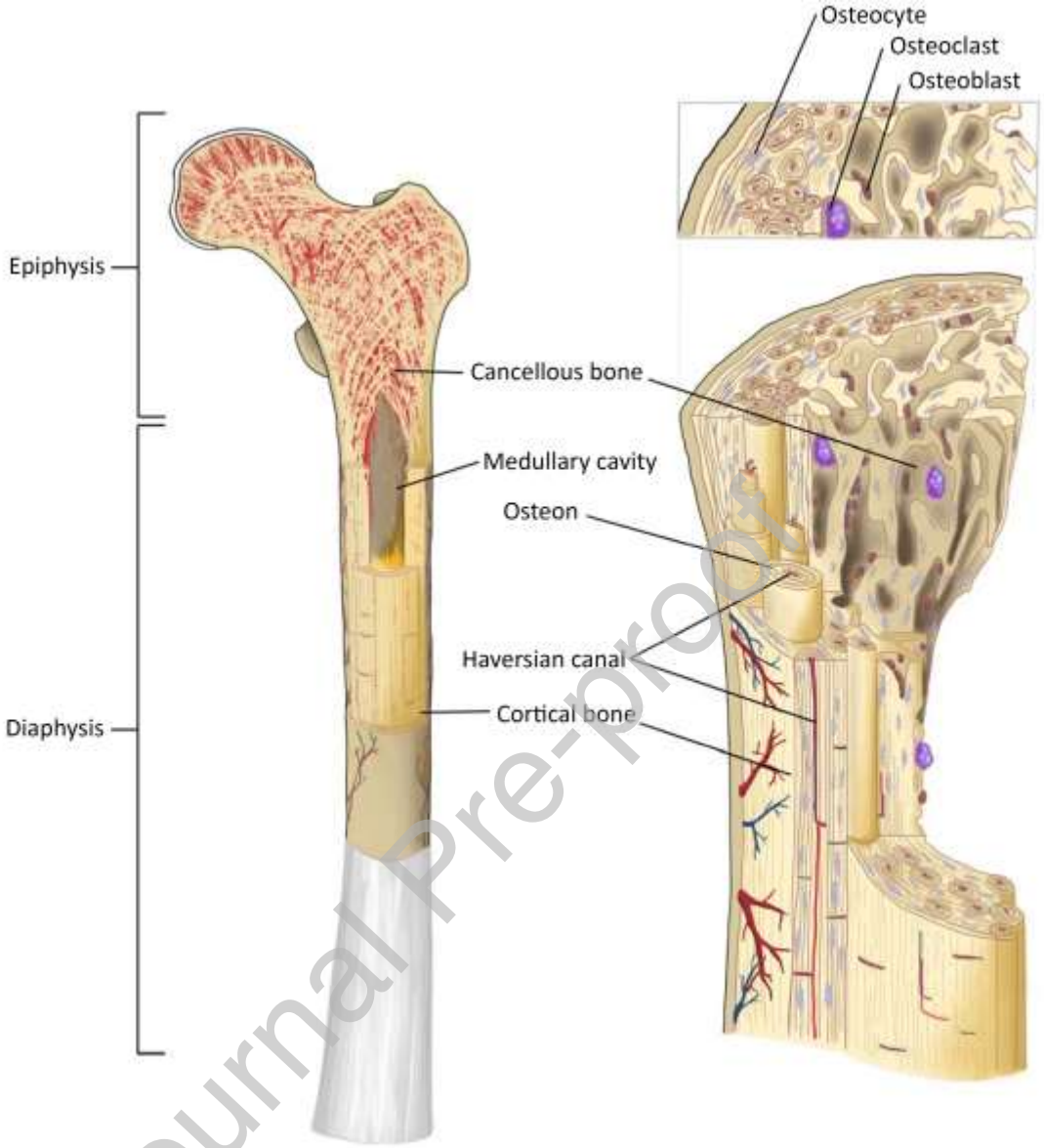

Figure 2

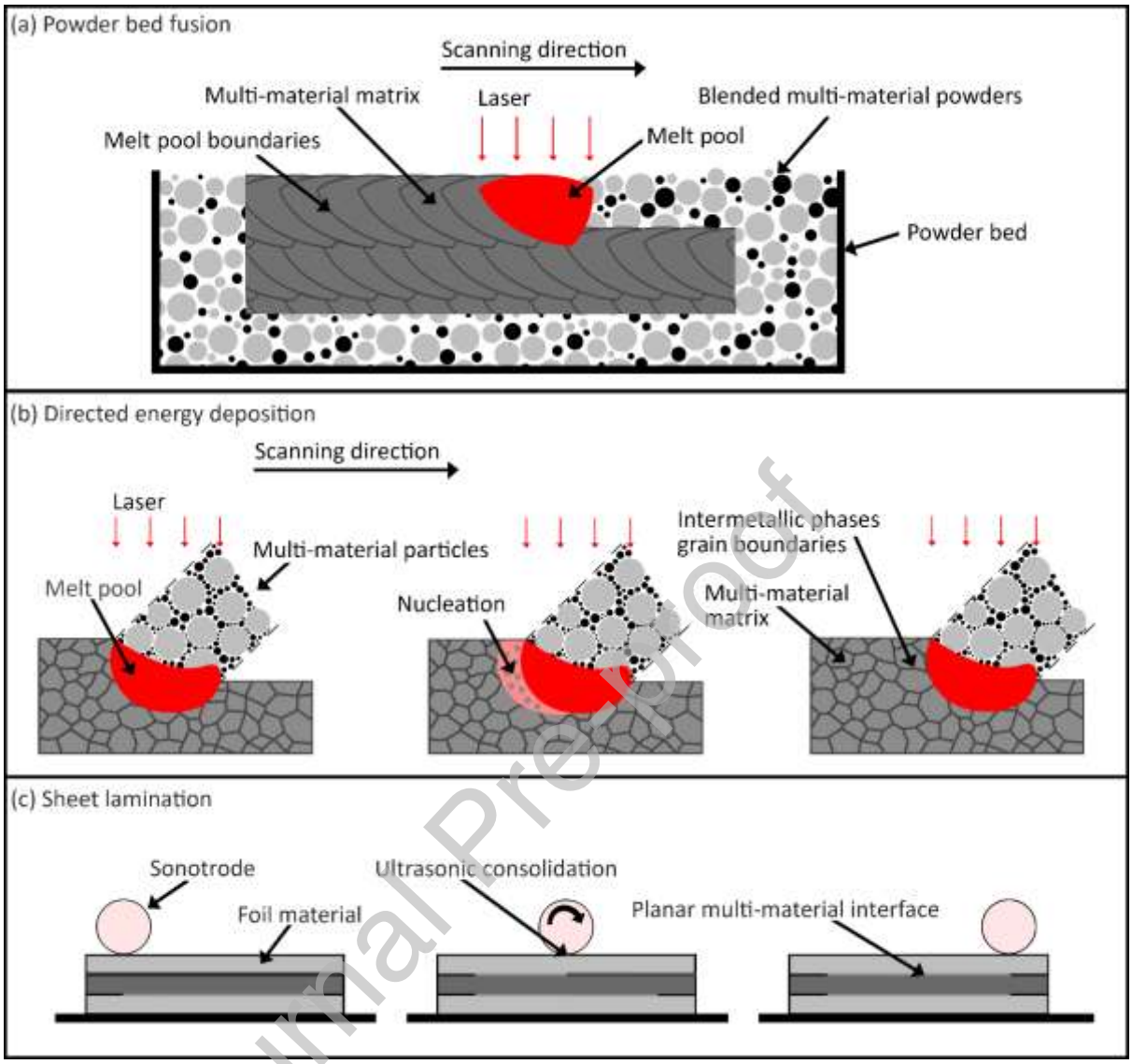

Figure 3

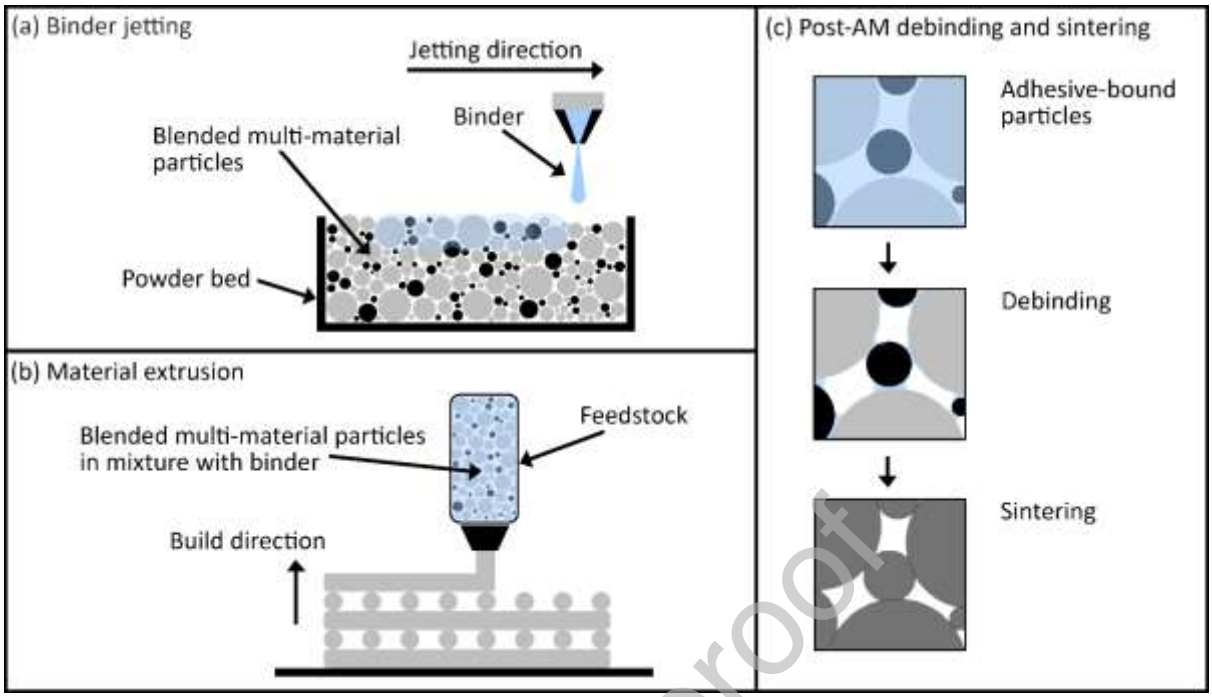

Figure 4

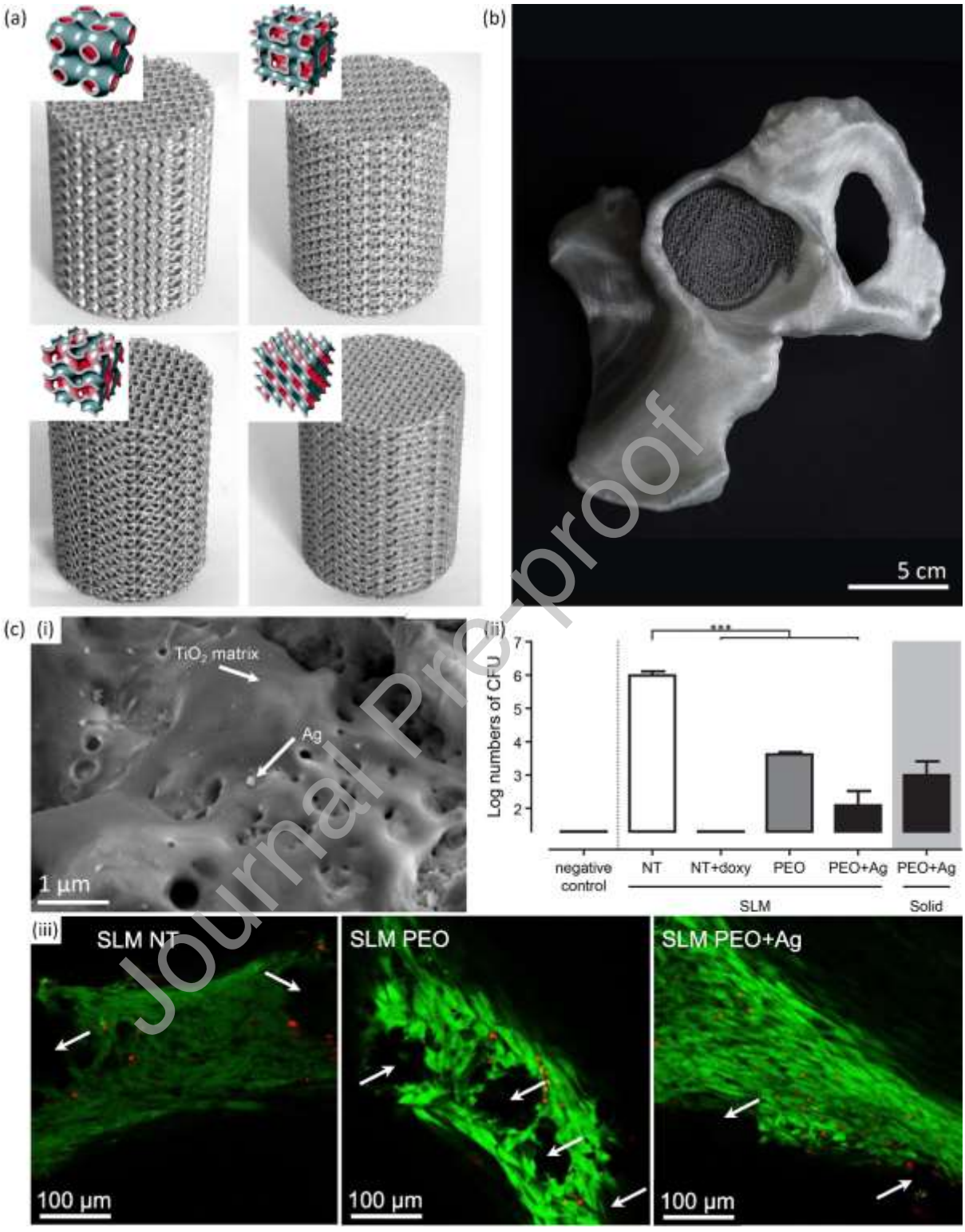

Figure 5

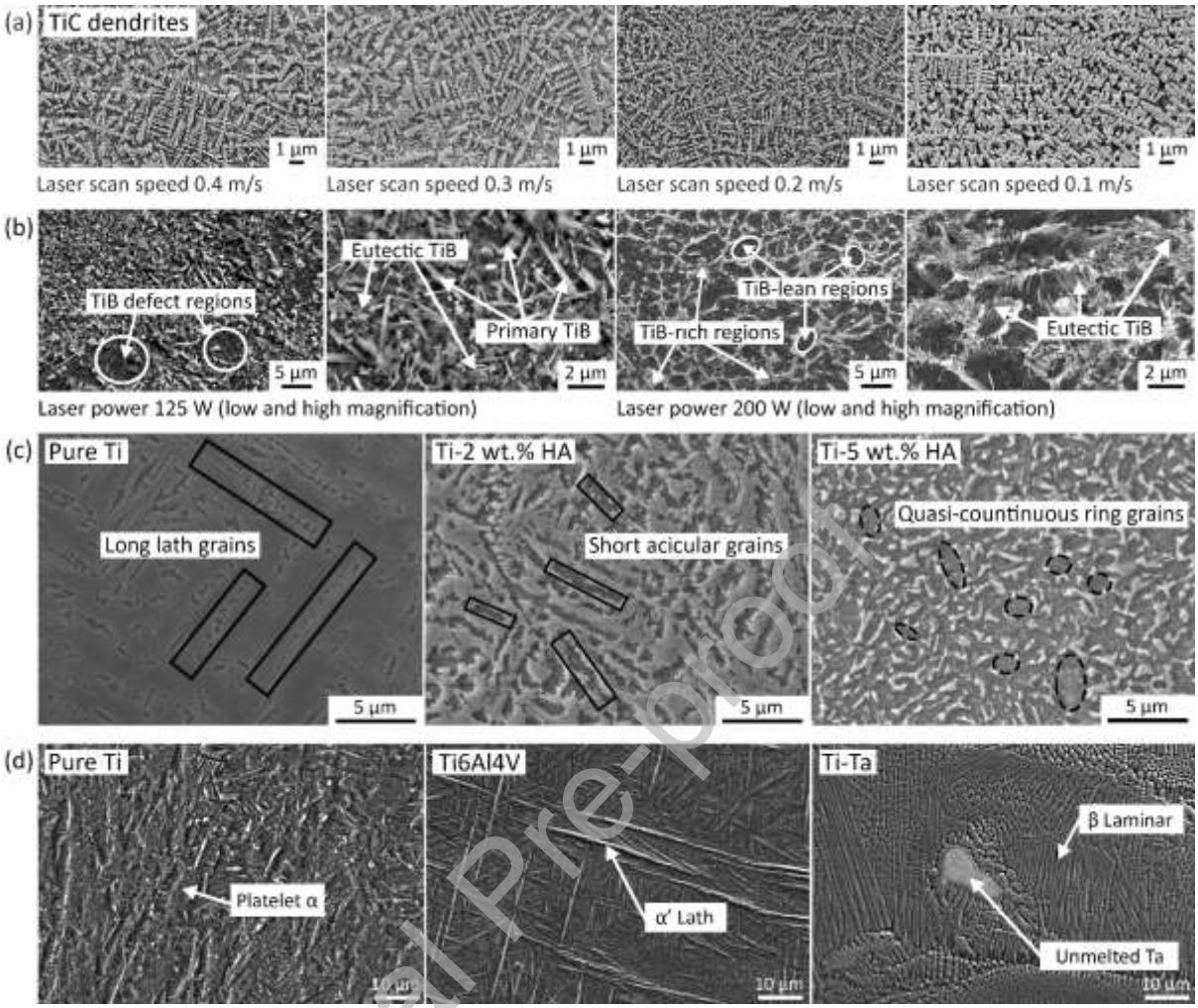

Figure 6

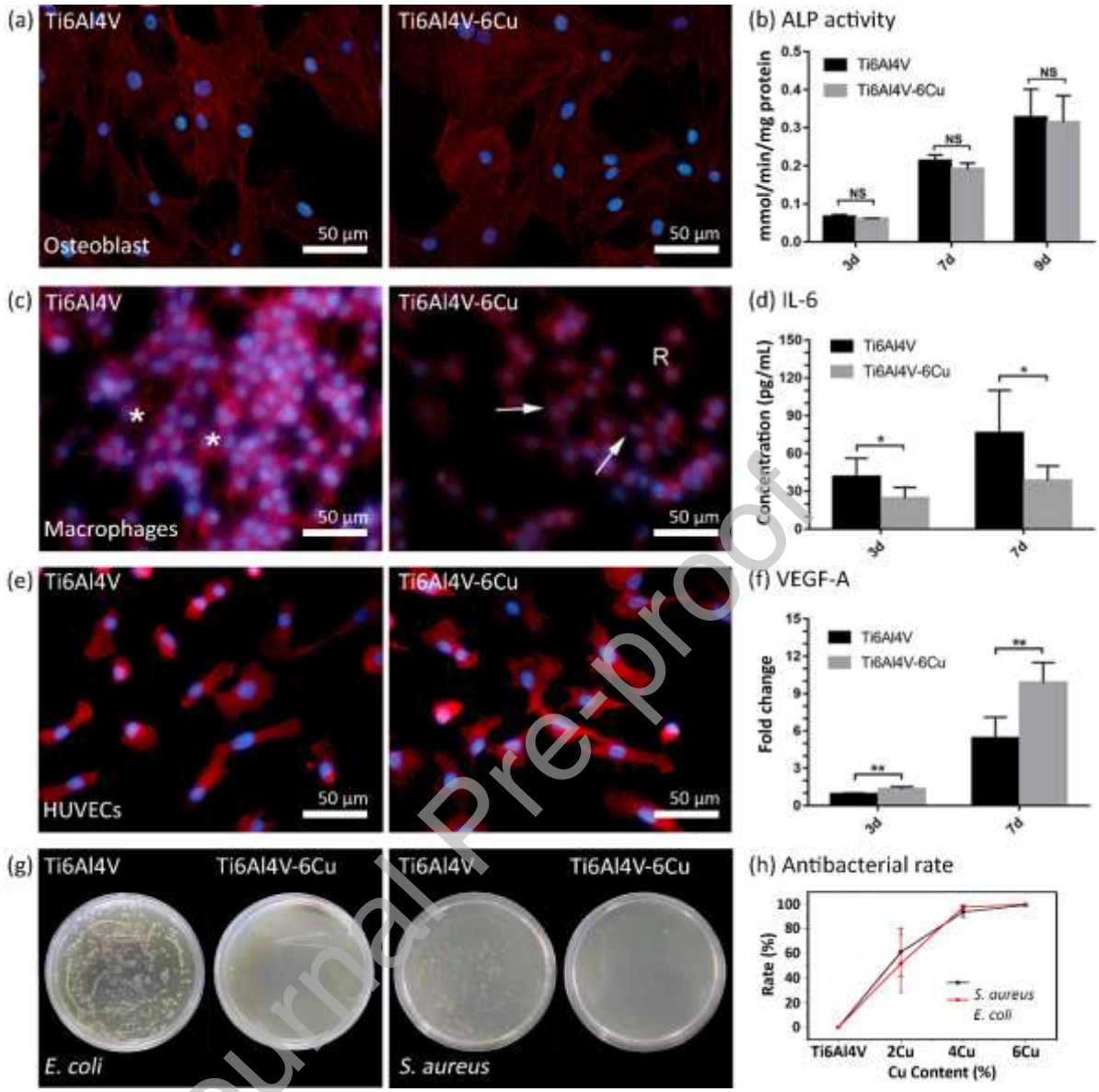

Figure 7

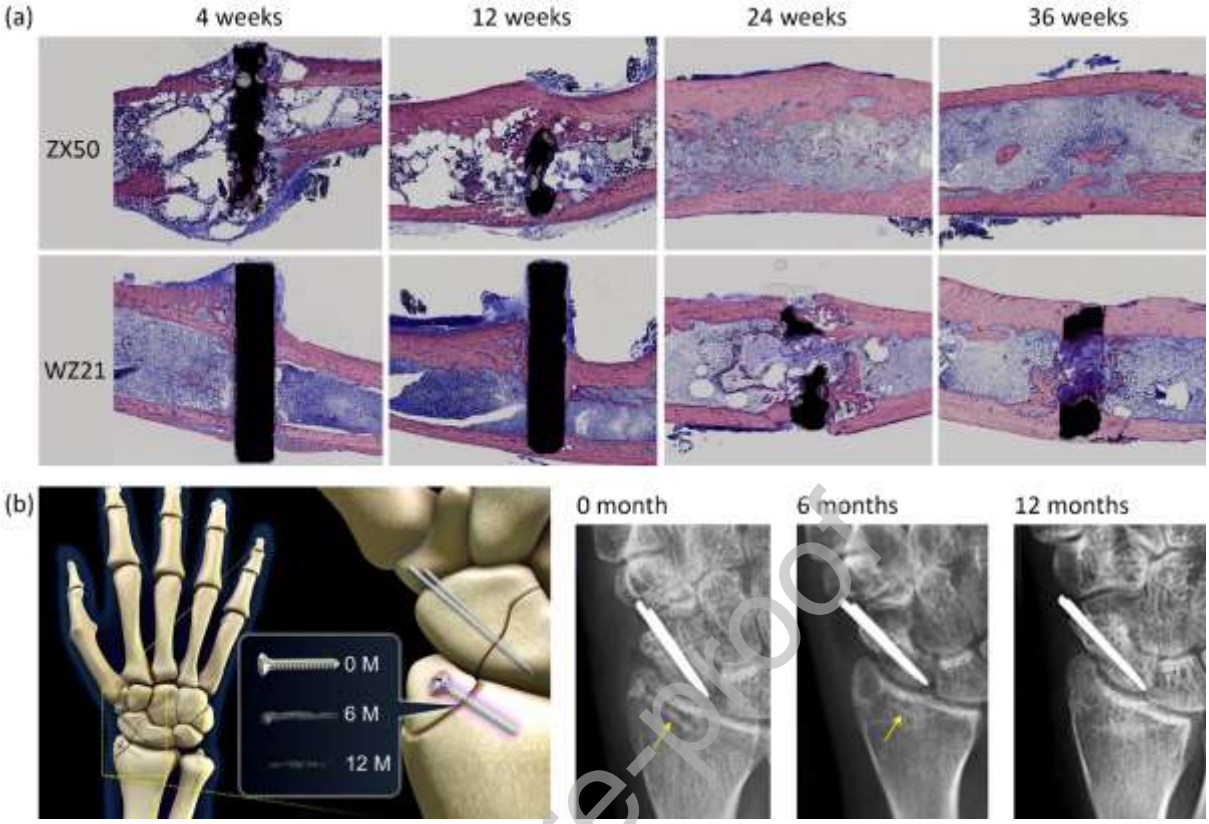

Figure 8

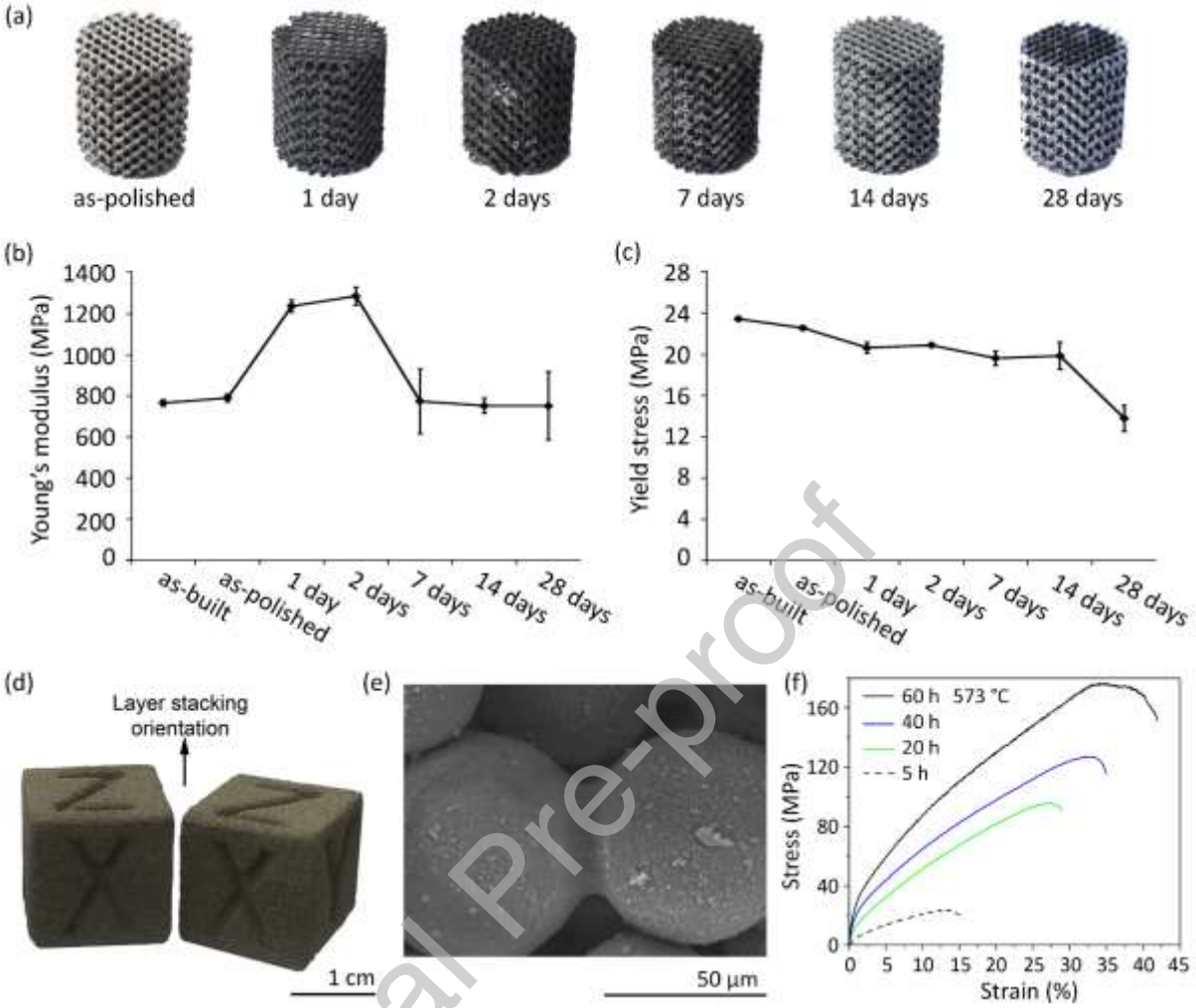

Figure 9

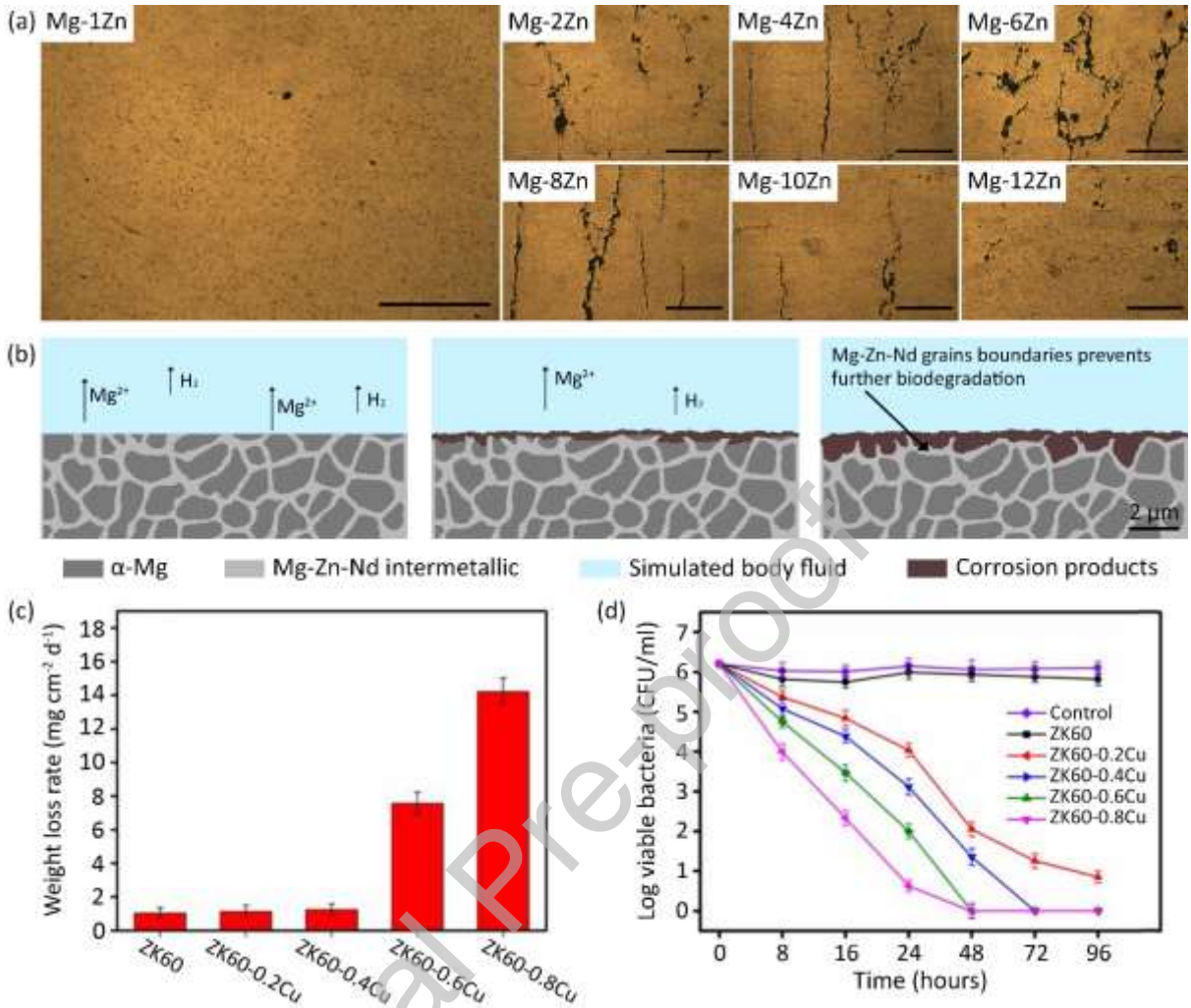

Figure 10

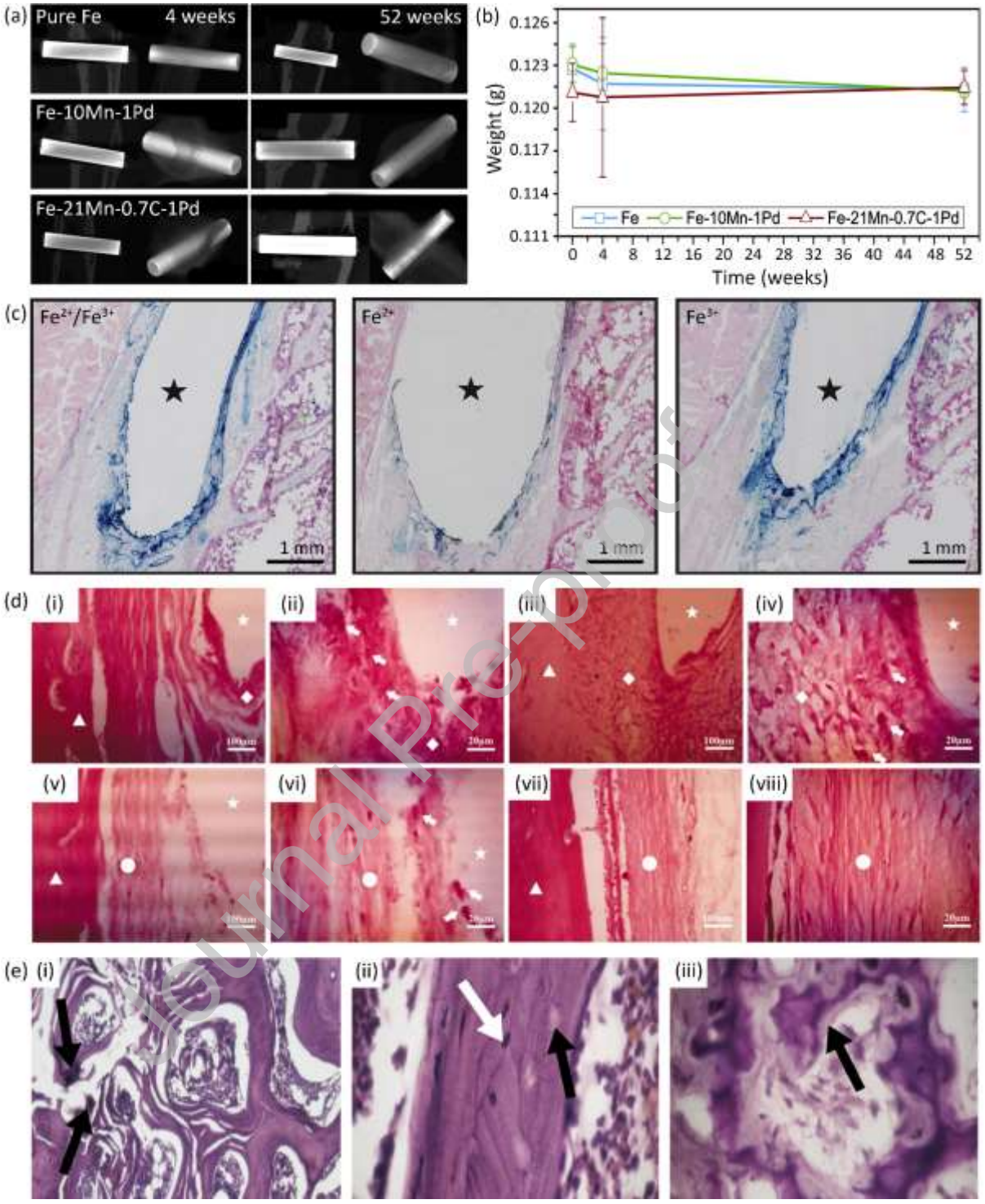

Figure 11

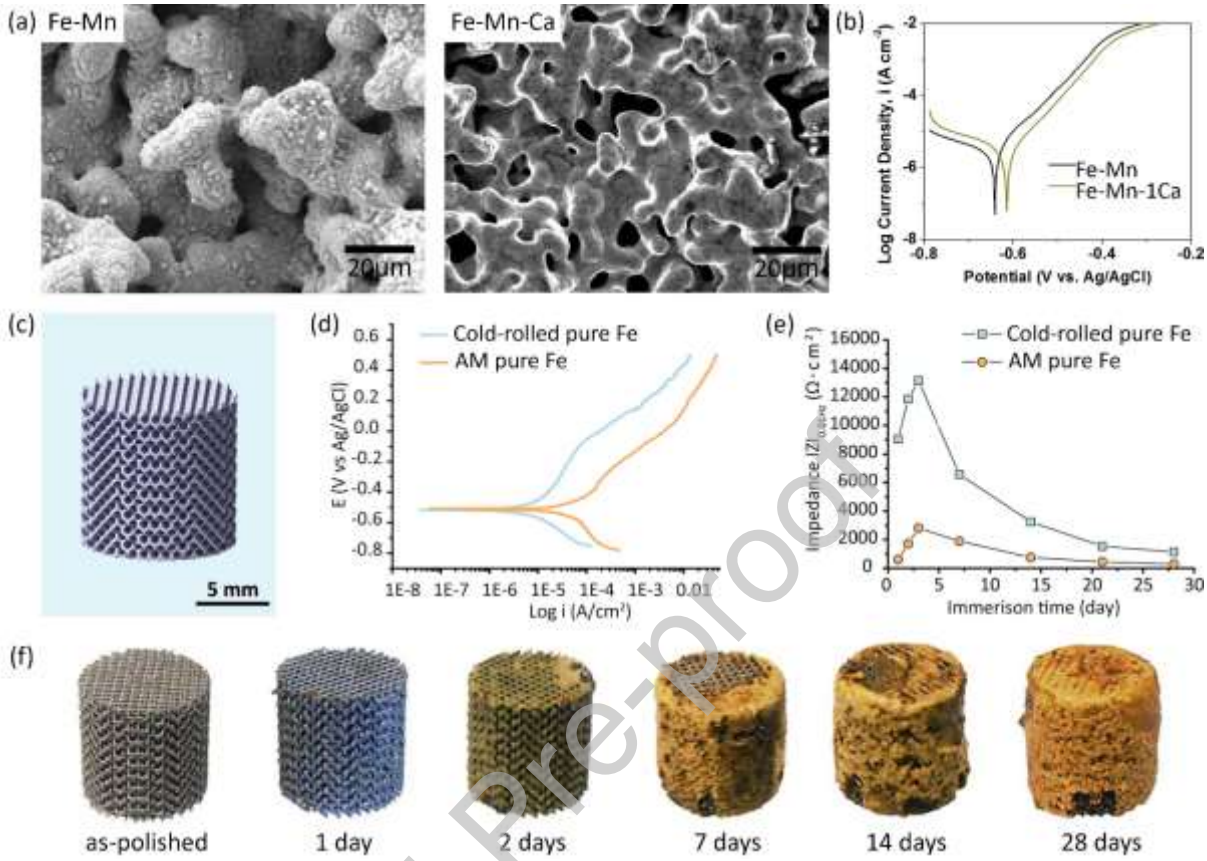

Figure 12

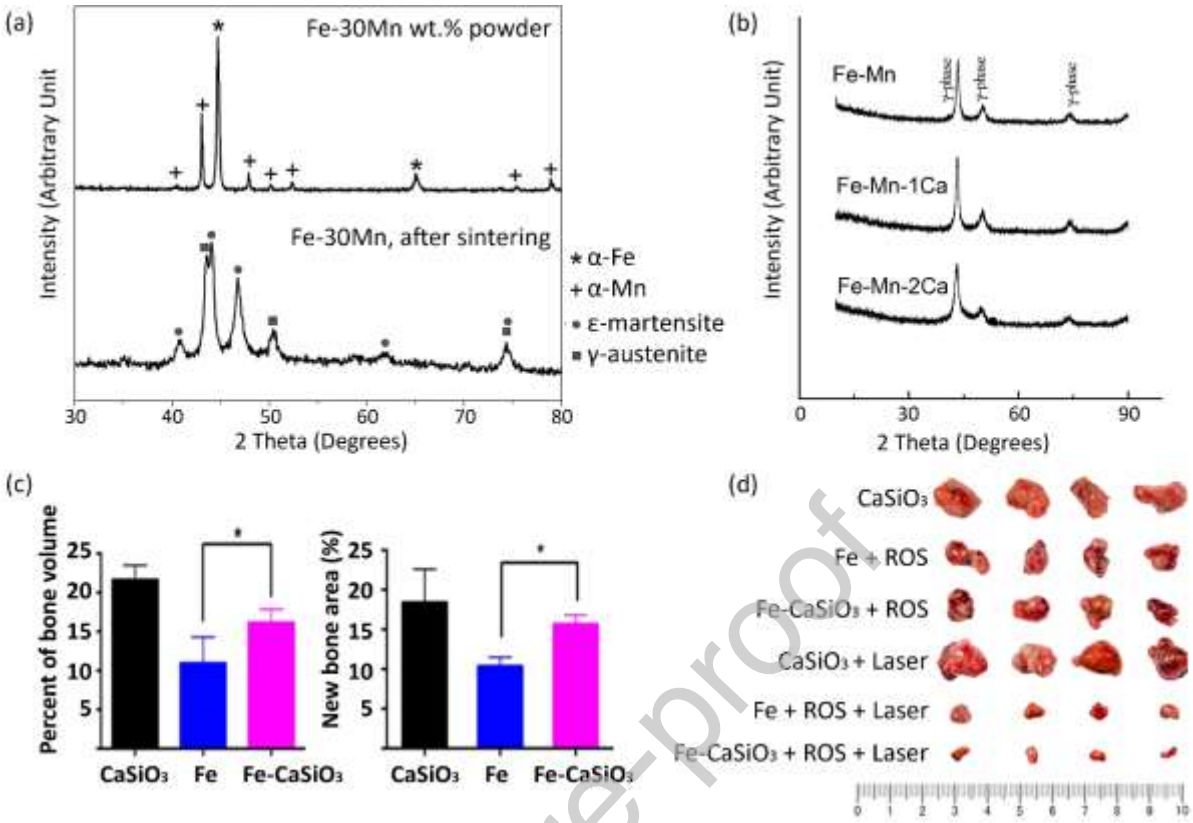

Graphical Abstract

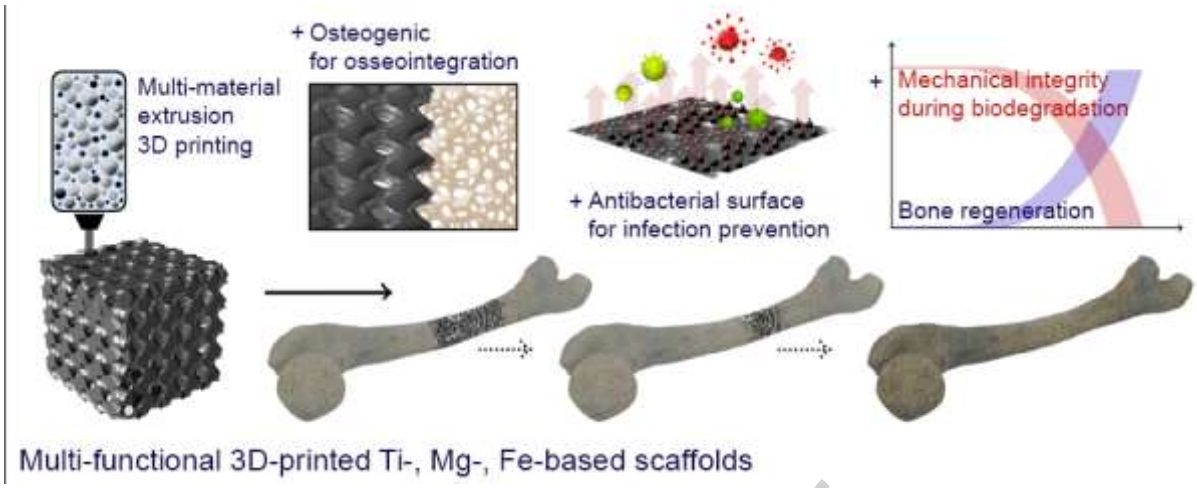

Declaration of interests

☒ The authors declare that they have no known competing financial interests or personal relationships that could have appeared to influence the work reported in this paper.

☐The authors declare the following financial interests/personal relationships which may be considered as potential competing interests: